

OPTIMIZED AND QUASI-OPTIMAL SCHWARZ WAVEFORM RELAXATION FOR THE ONE-DIMENSIONAL SCHRÖDINGER EQUATION

LAURENCE HALPERN

*Université Paris 13, LAGA, UMR CNRS 7539,
93430 Villetaneuse, France
halpern@math.univ-paris13.fr*

JÉRÉMIE SZEFTTEL

*Department of Mathematics,
Princeton University, Fine Hall, Washington Road,
Princeton, NJ 08544-1000, USA
and
Mathématiques Appliquées de Bordeaux,
Université Bordeaux 1, 351 cours de la Libération,
33405 Talence cedex, France
jszeftel@math.princeton.edu*

Received 7 November 2008

Revised 26 October 2009

Communicated by E. Zuazua

Schwarz waveform relaxation algorithms are designed for the linear Schrödinger equation with potential. Two classes of algorithms are introduced: the quasi-optimal algorithm, based on the transparent continuous or discrete boundary condition, and the optimized complex Robin algorithm. We analyze their properties in one dimension. First, well-posedness and convergence are studied, in the overlapping and the non-overlapping case, for constant or non-constant potentials. Then discrete algorithms are established, for which convergence is proved through discrete energies or Fourier transforms, as in the continuous case. Numerical results illustrate the efficiency of the methods, for various types of potentials and any number of subdomains.

Keywords: Domain decomposition methods; Schwarz waveform relaxation; Schrödinger equation; absorbing boundary conditions.

AMS Subject Classification: 35J10, 58J40, 65M12, 65M55

1. Introduction

The transient Schrödinger equation is the basic model in quantum mechanics. It is also the “parabolic approximation” of the wave equation, used in underwater acoustics, or in the so-called migration process, an imaging method to search for

hydrocarbons. The design of optical fibers, or new semiconductor devices is based on numerical simulations of a variety of such equations, linear with a potential, or nonlinear, or even part of a system, in large domains.³ Resolution is memory and time-consuming, therefore raising in a natural manner the need for domain decomposition. Even more important, discontinuities in the coefficients can be present, as in the earth for instance, or in semiconductors, and it would be useful to split the domain into different homogeneous subdomains, or even to couple different models.

New space-time domain decomposition algorithms for wave propagation or advection-diffusion problems have been developed recently, using two concepts: waveform relaxation, and optimized absorbing boundary conditions. This approach leads to efficient algorithms which solve the problem iteratively in each subdomain on the whole time interval (with possibly time windows), and exchange information on the boundary at the end of the time interval. At an early stage, Dirichlet transmission conditions were used with overlapping subdomains,⁹ but the convergence depends heavily on the overlap. Then it was realized that optimal convergence can be obtained when using transparent boundary operators as transmission operators between the subdomains. However, these operators are not available for general geometries and/or equations with variable coefficients. Therefore absorbing boundary conditions, with coefficients optimizing the convergence factor, have been used with or without overlap to improve this exchange of information, thus accelerating significantly the convergence. This idea was first developed for elliptic problems by Engquist and Zhao,⁷ and Nataf and co-authors.¹⁹ The optimization strategy in the frequency domain goes back to Japhet's thesis.¹³ For evolution problems, coupling these ideas with waveform relaxation leads to optimized Schwarz Waveform Relaxation (OSWR) algorithms.^{10,4} They can be used in a sequential or parallel way, and enable different space-time discretization in different subdomains. They also open potentiality for space-time refinement,¹¹ and act as preconditioners⁵ for the resolution of the original problem in an implicit time-discretization setting.

Here we intend to design fast Schwarz waveform relaxation algorithms for Schrödinger equations with a potential. A new formulation relies on the transparent boundary operator.¹ Since an exact representation of the transparent operator is available in one dimension as a convolution in time only, we restrict ourselves to the one-dimensional case. This case will give hints for the comparison between this "quasi-optimal" algorithm, and a more classical form with complex Robin transmission conditions, and contains nontrivial convergence proofs for the continuous and discrete algorithms. The reader interested in the setting of the algorithm with Dirichlet transmission conditions is referred to Halpern and Szeftel.¹²

After some preliminary results on Sobolev spaces in Sec. 2, optimal and quasi-optimal algorithms are introduced in Sec. 3. For a constant potential, we show that the overlapping and non-overlapping algorithms converge in two iterations for two subdomains. For a non-constant potential, we prove the convergence of the non-overlapping algorithm with energy estimates, following an idea of Desprès,⁶ which has widely been used since (see Nataf *et al.*¹⁹ for steady problems, Gander *et al.*¹⁰ for

evolution equations). Here, for the first time, it is extended to complex problems and pseudo-differential operators.

In Sec. 4, we introduce complex Robin type transmission conditions, and investigate the behavior of the corresponding algorithm. Such transmission conditions were first proposed by Lions¹⁶ for elliptic problems. We first prove the algorithms to be well-posed. For overlapping subdomains, we prove convergence of the algorithms for a constant potential, by Fourier transform in time and exact resolution of the equation in space. For non-overlapping subdomains, the proof involves energy estimates, and holds for a non-constant potential. We also study the optimization of the convergence factor for a constant potential.

In Sec. 5, the complex Robin algorithm is discretized with Finite Volumes. In the interior, it reduces to the Crank–Nicolson scheme, widely used in the linear and nonlinear computations for the Schrödinger equation, where the complex Robin transmission conditions are naturally taken into account. We also introduce a discretization of the quasi-optimal algorithm using the Crank–Nicolson scheme in the interior and the discrete transparent boundary condition designed by Arnold and Ehrhardt¹ precisely for the Crank–Nicolson scheme.

In Sec. 6, which is the most technical one, we tackle convergence issues. Using a discrete Laplace transform in time, we study the overlapping discrete algorithm with Robin type exchange of data, for a constant potential, for which the quasi-optimal algorithm converges in two iterations. The convergence of the non-overlapping complex Robin algorithm is proved with discrete energy estimates and holds for non-constant potentials.

In Sec. 7, we finally illustrate and extend the results through numerical simulations, for various types of potential, like constant, barrier or parabolic. For two subdomains, we show how slow the convergence is with Dirichlet transmission conditions, and how the optimized Schwarz waveform relaxation improves the convergence. We also show that the minimal number of iterations by far is obtained by the discrete quasi-optimal algorithm. To conclude, we show that convergence properties are preserved for any number of subdomains, and we discuss complexity issues.

Due to the complexity of the analysis, we restrain ourselves to the one-dimensional case. The multidimensional study contains additional difficulties due to the geometry and will be the heart of a forthcoming paper.

2. Model Problem and Function Spaces

Let V be a real potential in $L^\infty(\mathbb{R})$. We consider here the Schrödinger equation

$$\mathcal{L}u = i\partial_t u + \partial_{xx} u - Vu = f, \quad (2.1)$$

with the initial condition

$$u(x, 0) = u_0(x). \quad (2.2)$$

We first recall some definitions of functional spaces. Let Ω be an open subset of \mathbb{R} . The complex Hilbert space $L^2(\Omega)$ is equipped with the Hermitian product $(f, g) = \int_{\Omega} (f\bar{g})(x)dx$ and the corresponding norm $\|\cdot\|$. For r an integer, $H^r(\Omega)$ is the Sobolev space of distributions in $\mathcal{D}'(\Omega)$, whose derivatives of order up to r are in $L^2(\Omega)$, equipped with the norm $\|v\|_{H^r(\Omega)} = (\sum_{|\alpha|\leq r} \|D^\alpha v\|^2)^{1/2}$. If r is not an integer, the space $H^r(\Omega)$ is defined by interpolation. For the time direction, we will use another characterization. The Sobolev space $H^r(\mathbb{R})$ for real r is also the set of tempered distributions u in $\mathcal{S}'(\mathbb{R})$, whose Fourier transform \hat{u} is such that $(1 + \tau^2)^{r/2}\hat{u}$ is in $L^2(\mathbb{R})$. The space $H^r(\mathbb{R})$ is equipped with the norm $\|u\|_{H^r(\mathbb{R})} = \|(1 + \tau^2)^{r/2}\hat{u}\|$. Then $H^r([0, T])$ is the set of restrictions of elements in $H^r(\mathbb{R})$, and equipped with the quotient norm $\|u\|_{H^r([0, T])} = \inf\{\|U\|_{H^r(\mathbb{R})}, U = u \text{ a.e. in } (0, T)\}$. Note that if r is an integer, the second definition is equivalent to the first one, see Ref. 14.

We recall two classical *a priori* estimates. If u is a smooth solution to (2.1), (2.2) in $\mathbb{R} \times (0, T)$, then it satisfies for any positive time t the inequalities:

$$\frac{d}{dt} \|u(\cdot, t)\|^2 \leq \|f(\cdot, t)\|^2 + \|u(\cdot, t)\|^2, \tag{2.3}$$

$$\frac{d}{dt} \|\partial_x u(\cdot, t)\|^2 \leq \|f(\cdot, t)\|^2 + 2\|\partial_t u(\cdot, t)\|^2 + \|V\|_{L^\infty}^2 \|u(\cdot, t)\|^2. \tag{2.4}$$

There is an existence theorem in $L^2(0, T; H^1(\mathbb{R}))$ under convenient assumptions on u_0 and f , but the domain decomposition algorithms will require more regularity. Therefore we introduce now for any domain $\Omega \subset \mathbb{R}$ the anisotropic Sobolev spaces¹⁴

$$H^{r,s}(\Omega \times (0, T)) = L^2(0, T; H^r(\Omega)) \cap H^s(0, T; L^2(\Omega)). \tag{2.5}$$

If the initial value u_0 is in $H^2(\mathbb{R})$, if the real potential V is in $L^\infty(\mathbb{R})$, and if the right-hand side f is in $H^1(0, T; L^2(\mathbb{R}))$, then there exists a unique solution u to (2.1), (2.2) in $H^{2,1}(\mathbb{R} \times (0, T))$.

At the interfaces between subdomains, the Schwarz waveform relaxation algorithm will need traces of the subdomain approximations to the solution. Necessary trace and extension results can be found in the reference book, by Lions–Magenes.¹⁴

3. Quasi-Optimal Schwarz Waveform Relaxation Algorithm

We decompose the spatial domain $\Omega = \mathbb{R}$ into two subdomains $\Omega_1 = (-\infty, L)$ and $\Omega_2 = (0, \infty)$, with $L \geq 0$. The Schwarz waveform relaxation algorithm consists in solving iteratively subproblems on $\Omega_1 \times (0, T)$ and $\Omega_2 \times (0, T)$, using as a boundary condition at the interfaces $\Gamma_1 = \{x = L\}$ and $\Gamma_2 = \{x = 0\}$ values obtained from the previous iteration in the neighboring subdomain. For any operators \mathcal{B}_1 and \mathcal{B}_2 , we define the algorithm for $k \geq 1$ by

$$\begin{aligned} \mathcal{L}u_1^k &= f \quad \text{in } \Omega_1 \times (0, T), & \mathcal{L}u_2^k &= f \quad \text{in } \Omega_2 \times (0, T), \\ u_1^k(\cdot, 0) &= u_0 \quad \text{in } \Omega_1, & u_2^k(\cdot, 0) &= u_0 \quad \text{in } \Omega_2, \\ \mathcal{B}_1 u_1^k &= \mathcal{B}_1 u_2^{k-1} \quad \text{on } \Gamma_1 \times (0, T), & \mathcal{B}_2 u_2^k &= \mathcal{B}_2 u_1^{k-1} \quad \text{on } \Gamma_2 \times (0, T). \end{aligned} \tag{3.1}$$

An initial guess (g_1, g_2) is given on the boundary, and the zero iterate is given by $\mathcal{B}_1 u_2^0 \equiv g_1, \mathcal{B}_2 u_1^0 \equiv g_2$. The case where both operators \mathcal{B}_j are the identity and the transmission condition in domain 2 is $u_2^k = u_1^k$ has been defined in previous works as *classical* or *alternate* Schwarz, referring to the seminal work by Schwarz²¹ on the Poisson equation in a multiple domain. It has been used for numerical domain decomposition for a long time, in the alternate or parallel version,¹⁵ and has been analyzed in the context of Schwarz waveform relaxation for the advection-diffusion by Gander and Zhao,⁹ and for the wave equation in Gander and Halpern.⁸ It is known to converge if a certain amount of overlap is present, but the convergence is very slow. For a study of that algorithm for the Schrödinger equation, we refer the interested reader to Halpern and Szeftel.¹² We will give some numerical comparisons in Sec. 7.

3.1. Optimal transmission conditions

We will search operators \mathcal{B}_j in a special class, related to the Dirichlet–Neumann map. They are given by $\mathcal{B}_j = \partial_x + \mathcal{S}_j, j = 1, 2$, where the $\mathcal{S}_j(\partial_t)$ are pseudo-differential operators in time, with symbol σ_j defined by the following formula, where $\hat{\cdot}$ denotes the Fourier transform in time.

$$\mathcal{S}_j \phi(t) = (2\pi)^{-1/2} \int e^{i\tau t} \sigma_j(\tau) \hat{\phi}(\tau) d\tau.$$

Theorem 3.1. *Let V be a real constant. The sequence of iterates (u_1^k, u_2^k) in algorithm (3.1) converges to the solution u to (2.1), (2.2) in two iterations for every initial guess (g_1, g_2) , independently of the size of the overlap $L \geq 0$, if and only if the operators \mathcal{S}_1 and \mathcal{S}_2 have the corresponding symbols*

$$\sigma_1 = (\tau + V)^{1/2}, \quad \sigma_2 = -(\tau + V)^{1/2}, \tag{3.2}$$

with

$$(\tau + V)^{1/2} = \begin{cases} \sqrt{\tau + V} & \text{if } \tau + V \geq 0, \\ -i\sqrt{-\tau - V} & \text{if } \tau + V < 0. \end{cases} \tag{3.3}$$

Proof. We use the Fourier transform in time with parameter τ . By linearity it suffices to prove the convergence to zero of the iterates associated with $f = 0$ and $u_0 = 0$. We can Fourier transform the equation in time and we get

$$\partial_{xx} \widehat{u}_j^k - (\tau + V) \widehat{u}_j^k = 0,$$

which can be solved as

$$\widehat{u}_1^k(x, \tau) = \alpha(\tau) e^{-(\tau+V)^{1/2}(L-x)}, \quad \widehat{u}_2^k(x, \tau) = \beta(\tau) e^{-(\tau+V)^{1/2}x}.$$

With the general transmission conditions in (3.1), we can write

$$\begin{aligned} ((\tau + V)^{1/2} + \sigma_1)\widehat{u}_1^2(L, \tau) &= -(\tau + V)^{1/2} + \sigma_1)\widehat{u}_1^1(L, \tau), \\ -(\tau + V)^{1/2} + \sigma_2)\widehat{u}_2^2(0, \tau) &= ((\tau + V)^{1/2} + \sigma_2)\widehat{u}_1^1(0, \tau). \end{aligned}$$

Now $(\widehat{u}_1^2(L, \tau), \widehat{u}_2^2(0, \tau))$ vanish for any initial guess, if and only if $-(\tau + V)^{1/2} + \sigma_1 = (\tau + V)^{1/2} + \sigma_2 = 0$. □

We call these operators optimal, since they lead to convergence in two iterations for any initial guess. For variable potentials, the optimal operators are in general not at hand. We present here and compare two approximations of those. The first one is a “frozen coefficients” variant of these operators. The second one replaces them by a constant, obtaining “Robin type” transmission conditions, and finds the constant by minimizing the convergence factor.

3.2. The quasi-optimal algorithm

We use as transmission operators the optimal operators for the constant potential equal to the value of V on the interface. The quasi-optimal algorithm is thus given by

$$\mathcal{S}_1^{\text{qo}} = \sqrt{-i\partial_t + V(L)}, \quad \mathcal{S}_2^{\text{qo}} = -\sqrt{-i\partial_t + V(0)}, \quad \mathcal{B}_j^{\text{qo}} = \partial_x + \mathcal{S}_j^{\text{qo}}, \quad (3.4)$$

where $\sqrt{-i\partial_t + V(x)}$ is the operator acting only in time with symbol $(\tau + V(x))^{1/2}$. Though being not differential, this operator is still easy to use numerically.¹

We call the algorithm with transmission operators (3.4) quasi-optimal, in the sense that it is optimal for a constant potential, with or without overlap, according to Theorem 3.1. For a constant potential, the proof of well-posedness relies on Fourier transform in time and exact computation of the solution. We do not have a proof of well-posedness in the case where V is a variable potential. On the other hand, we are able to prove the convergence of the non-overlapping algorithm, i.e. $L = 0$, and when $T = +\infty$. The proof is based on energy estimates and follows an idea of Després,⁶ which has widely been used since. The first extension to time-dependent problems was to the one-dimensional wave equations.¹⁰ Here it is extended to pseudo-differential operators for the first time.

Theorem 3.2. *Let $L = 0$. Let the potential V be such that V and V' belong to $L^\infty(\mathbb{R})$. Then the iterates (u_1^k, u_2^k) of algorithm (3.1) with transmission operators (3.4) converge to the solution to (2.1), (2.2) in $(H^{1/4}(0, T, L^2(\Omega_1)) \cap H^{-1/4}(0, T, H^1(\Omega_1))) \times (H^{1/4}(0, T, L^2(\Omega_2)) \cap H^{-1/4}(0, T, H^1(\Omega_2)))$.*

Remark 3.1. The assumption $V' \in L^\infty(\mathbb{R})$ is very strong and not suitable for some of the applications mentioned in the Introduction. In particular, such an assumption forbids any slow tunnel effect for the Schrödinger equation (2.1). However, we believe that this assumption is purely technical and that convergence should hold even without it. This belief is supported by our numerical results (see Sec. 7) which exhibit fast convergence even in the case of a potential barrier.

Proof. By linearity it suffices to prove the convergence to zero of the iterates associated with vanishing right-hand side and initial values. Since $L = 0$, we have $\mathcal{S}_1^{q_0} = -\mathcal{S}_2^{q_0}$, and we denote this operator by \mathcal{S} . Consider the equation on the whole range of times $0 \leq t < +\infty$ with the boundary conditions

$$(\partial_x + \mathcal{S})u_1^k(0, \cdot) = (\partial_x + \mathcal{S})u_2^{k-1}(0, \cdot), \quad (\partial_x - \mathcal{S})u_2^k(0, \cdot) = (\partial_x - \mathcal{S})u_1^{k-1}(0, \cdot). \tag{3.5}$$

We introduce $\eta > 0$ satisfying

$$\eta \geq \|V'\|_{L^\infty(\mathbb{R})}^{2/3}. \tag{3.6}$$

Let U_j^k be the extension of $e^{-\eta t}u_j^k$ to $\Omega_j \times \mathbb{R}$ vanishing on $\Omega_j \times (-\infty, 0)$. For any x , we define the operator $\mathcal{S}_\eta(x) = \sqrt{-i\partial_t + V(x) - i\eta}$. It satisfies

$$e^{-\eta t}\mathcal{S}e^{\eta t} = \mathcal{S}_\eta.$$

For $k \geq 1, U_j^k, j = 1, 2$, satisfy the equations

$$\begin{cases} (i\partial_t + \partial_{xx} - V + i\eta)U_1^k = 0 & \text{in } \Omega_1 \times \mathbb{R}, \\ \mathcal{B}_1 U_1^k(0, \cdot) = \mathcal{B}_1 U_2^{k-1}(0, \cdot) & \text{in } \mathbb{R}, \end{cases} \quad \begin{cases} (i\partial_t + \partial_{xx} - V + i\eta)U_2^k = 0 & \text{in } \Omega_2 \times \mathbb{R}, \\ \mathcal{B}_2 U_2^k(0, \cdot) = \mathcal{B}_2 U_1^{k-1}(0, \cdot) & \text{in } \mathbb{R}, \end{cases} \tag{3.7}$$

where the transmission operators \mathcal{B}_j are given by $\mathcal{B}_1 = \partial_x + \mathcal{S}_\eta(0)$, and $\mathcal{B}_2 = \partial_x - \mathcal{S}_\eta(0)$. For fixed $x, \sigma_\eta(x) = (\tau + V(x) - i\eta)^{1/2}$ is the unique analytic determination of the square root with positive real part (and hence negative imaginary part). Multiplying the equation for U_1^k in (3.7) by $\overline{\mathcal{S}_\eta(x)U_1^k}$, taking the real part, integrating in time, and integrating by parts in space yields

$$\begin{aligned} & \mathcal{R}e \int_{\mathbb{R}} \int_{-\infty}^0 \mathcal{S}_\eta^2(x)U_1^k \overline{\mathcal{S}_\eta(x)U_1^k} dx dt + \mathcal{R}e \int_{\mathbb{R}} \int_{-\infty}^0 \mathcal{S}_\eta(x)\partial_x U_1^k \overline{\partial_x U_1^k} dx dt \\ & - \mathcal{R}e \int_{\mathbb{R}} \partial_x U_1^k(0, \cdot) \overline{\mathcal{S}_\eta(0)U_1^k(0, \cdot)} dt = \frac{1}{2} \mathcal{R}e \int_{\mathbb{R}} \int_{-\infty}^0 V'(x)\partial_x U_1^k \overline{(\mathcal{S}_\eta(x))^{-1}U_1^k} dx dt. \end{aligned} \tag{3.8}$$

By using the Plancherel identity in time and

$$\mathcal{R}e(a\bar{b}) = \frac{1}{4}(|a + b|^2 - |a - b|^2)$$

we obtain:

$$\begin{aligned} & \int_{\mathbb{R}} \int_{-\infty}^0 \mathcal{R}e(\sigma_\eta(x))|\sigma_\eta(x)|^2|\widehat{U}_1^k(\tau, x)|^2 dx d\tau \\ & + \int_{\mathbb{R}} \int_{-\infty}^0 \mathcal{R}e(\sigma_\eta(x))|\partial_x \widehat{U}_1^k(\tau, x)|^2 dx d\tau + \frac{1}{4} \int_{\mathbb{R}} |\partial_x U_1^k(0, \cdot) - \mathcal{S}_\eta(0)U_1^k(0, \cdot)|^2 dt \end{aligned}$$

$$\begin{aligned} &\leq \frac{1}{4} \int_{\mathbb{R}} |\partial_x U_1^k(0, \cdot) + \mathcal{S}_\eta(0) U_1^k(0, \cdot)|^2 dt \\ &\quad + \frac{1}{2} \|V'\|_{L^\infty} \int_{\mathbb{R}} \int_{-\infty}^0 |\sigma_\eta(x)|^{-1} |\partial_x \widehat{U}_1^k(\tau, x)| |\widehat{U}_1^k(\tau, x)| dx d\tau. \end{aligned} \tag{3.9}$$

We have an upper bound for the last term by

$$\begin{aligned} &\frac{1}{2} \int_{\mathbb{R}} \int_{-\infty}^0 \operatorname{Re}(\sigma_\eta(x)) |\partial_x \widehat{U}_1^k(\tau, x)|^2 dx d\tau \\ &\quad + \frac{1}{8} \|V'\|_{L^\infty}^2 \int_{\mathbb{R}} \int_{-\infty}^0 \frac{|\widehat{U}_1^k(\tau, x)|^2}{\operatorname{Re}(\sigma_\eta(x)) |\sigma_\eta(x)|^2} dx d\tau. \end{aligned} \tag{3.10}$$

Now since

$$\operatorname{Re}(\sigma_\eta(x)) = \left(\frac{\tau + V(x) + |\sigma_\eta(x)|^2}{2} \right)^{1/2},$$

we get

$$\operatorname{Re}(\sigma_\eta(x)) \geq \frac{\eta}{2} |\sigma_\eta(x)|^{-1}, \tag{3.11}$$

which in turn yields

$$(\operatorname{Re}(\sigma_\eta(x)) |\sigma_\eta(x)|^2)^2 \geq \frac{\eta^2 |\sigma_\eta(x)|^2}{4} \geq \frac{\eta^3}{4}.$$

Therefore:

$$\begin{aligned} \frac{\|V'\|_{L^\infty}^2}{8} \frac{1}{\operatorname{Re}(\sigma_\eta(x)) |\sigma_\eta(x)|^2} &\leq \frac{\|V'\|_{L^\infty}^2}{2\eta^3} \operatorname{Re}(\sigma_\eta(x)) |\sigma_\eta(x)|^2 \\ &\leq \frac{1}{2} \operatorname{Re}(\sigma_\eta(x)) |\sigma_\eta(x)|^2, \end{aligned} \tag{3.12}$$

where we have used (3.6) to get the last inequality. Thus, using (3.9), (3.10) and (3.12) we obtain:

$$\begin{aligned} &\int_{\mathbb{R}} \int_{-\infty}^0 \operatorname{Re}(\sigma_\eta(x)) |\sigma_\eta(x)|^2 |\widehat{U}_1^k(\tau, x)|^2 dx d\tau \\ &\quad + 2 \int_{\mathbb{R}} \int_{-\infty}^0 \operatorname{Re}(\sigma_\eta(x)) |\partial_x \widehat{U}_1^k(\tau, x)|^2 dx d\tau \\ &\quad + \frac{1}{2} \int_{\mathbb{R}} |(\partial_x - \mathcal{S}_\eta(0)) U_1^k(0, \cdot)|^2 dt \\ &\leq \frac{1}{2} \int_{\mathbb{R}} |(\partial_x + \mathcal{S}_\eta(0)) U_1^k(0, \cdot)|^2 dt. \end{aligned} \tag{3.13}$$

Introducing the energy in domain Ω_j

$$\begin{aligned}
 J_j(w) &= \int_{\mathbb{R}} \int_{\Omega_j} \operatorname{Re}(\sigma_\eta(x)) |\sigma_\eta(x)|^2 |\widehat{w}(\tau, x)|^2 dx d\tau \\
 &\quad + 2 \int_{\mathbb{R}} \int_{\Omega_j} \operatorname{Re}(\sigma_\eta(x)) |\widehat{\partial_x w}(\tau, x)|^2 dx d\tau,
 \end{aligned}
 \tag{3.14}$$

we can rewrite (3.13) as

$$J_1(U_1^k) + \frac{1}{2} \int_{\mathbb{R}} |\mathcal{B}_2 U_1^k|^2 dt \leq \frac{1}{2} \int_{\mathbb{R}} |\mathcal{B}_1 U_1^k|^2 dt.
 \tag{3.15}$$

Similarly, we obtain for U_2^k

$$J_2(U_2^k) + \frac{1}{2} \int_{\mathbb{R}} |\mathcal{B}_1 U_2^k|^2 dt \leq \frac{1}{2} \int_{\mathbb{R}} |\mathcal{B}_2 U_2^k|^2 dt.
 \tag{3.16}$$

Introducing the transmission conditions in the right-hand side of Eqs. (3.15) and (3.16), adding and summing in k , we find

$$\begin{aligned}
 &\sum_{k=1}^K (J_1(U_1^k) + J_2(U_2^k)) + \frac{1}{2} \int_{\mathbb{R}} (|\mathcal{B}_2 U_1^K|^2 + |\mathcal{B}_1 U_2^K|^2) dt \\
 &\leq \frac{1}{2} \int_{\mathbb{R}} (|\mathcal{B}_2 U_1^0|^2 + |\mathcal{B}_1 U_2^0|^2) dt.
 \end{aligned}
 \tag{3.17}$$

The sum of the energies over all the iterates remains bounded. Hence the energy $J_1(U_1^k) + J_2(U_2^k)$ needs to tend to zero.

Finally, using (3.11) and the definitions of J_1 and J_2 , we see that there exists a constant $C > 0$ depending on η and $\|V\|_{L^\infty(\mathbb{R})}$ such that

$$J_j(w) \geq C(\|w\|_{H^{1/4}(0,T,L^2(\Omega_j))}^2 + \|\partial_x w\|_{H^{-1/4}(0,T,L^2(\Omega_j))}^2).$$

Therefore, algorithm (3.4) converges in $\Pi_{j=1,2} L^2((0, T) \times \Omega_j) \cap H^{-1/4}(0, T, H^1(\Omega_j))$. \square

Remark 3.2. The previous proof does not provide any convergence rate. Now, the quasi-optimal algorithm (3.4) uses the optimal transmission conditions for a frozen potential. Thus, to obtain such convergence rates, one may consider the particular case of slowly varying potentials. After a unitary change of scale, the problem reduces to the study of operators of type $h^2 \partial_{xx} - V(x)$ for a small parameter $h > 0$, for which one may use tools coming from the semiclassical analysis. We refer the reader to Nataf and Nier¹⁸ for an application of the semiclassical calculus to domain decomposition methods for advection-diffusion equations.

4. The Algorithm with Complex Robin Transmission Conditions

A simpler alternative to the previous approach is to use Robin transmission conditions. This idea was first suggested by Lions¹⁵ in the context of elliptic problems.

Since the Schrödinger equation has complex coefficients, we choose a complex Robin algorithm rather than the usual Robin algorithm, i.e. we replace the optimal operators, for a real number p , by

$$\mathcal{S}_1^r = -\mathcal{S}_2^r = -ipI, \quad \mathcal{B}_j^r = \partial_x + \mathcal{S}_j^r. \tag{4.1}$$

Remark 4.1. In the sequel, we will choose $p > 0$ to ensure well-posedness and convergence of the algorithm (see Secs. 4.1–4.4).

4.1. Well-posedness of the algorithm

The algorithm is well-defined, provided the initial boundary value problems in each subdomain are well-posed. Those are non-classical problems, which need a special treatment. The following proposition gives existence, uniqueness and regularity of the solution.

Proposition 4.1. *Let the real potential V be in $L^\infty(\Omega)$. Suppose f is in $H^1(0, T; L^2(\Omega))$, u_0 in $H^2(\Omega)$, g_1 and g_2 are in $H^1(0, T)$, with the compatibility conditions*

$$\mathcal{B}_1^r u_0(L) = g_1(0), \quad \mathcal{B}_2^r u_0(0) = g_2(0). \tag{4.2}$$

Then, for $p > 0$, the boundary value problems (3.1) with Robin transmission operators (4.1) have unique solutions u_j in $H^{2,1}(\Omega_j \times (0, T))$.

Furthermore, assume $L = 0$. Then $u_j(0, \cdot)$ and $\partial_x u_j(0, \cdot)$ are in $H^1(0, T)$ and the following compatibility relation is satisfied:

$$\lim_{t \rightarrow 0_+} \mathcal{B}_2^r u_1(0, t) = \mathcal{B}_2^r u_0(0), \quad \lim_{t \rightarrow 0_+} \mathcal{B}_1^r u_2(L, t) = \mathcal{B}_1^r u_0(L). \tag{4.3}$$

The same conclusion holds when $L > 0$ provided that V is constant, f is in $H^2((0, T) \times \Omega)$ and u_0 is in $H^4(\Omega)$.

Proof. Without loss of generality, we only study the well-posedness of the subdomain problem in Ω_1 .

(i) First *a priori* estimates. Multiplying the equation $\mathcal{L}u_1 = f$ by \bar{u}_1 , integrating by parts in space, using the boundary condition and taking the imaginary part, we obtain

$$\frac{1}{2} \frac{d}{dt} \|u_1(\cdot, t)\|^2 + p|u_1(L, t)|^2 = \mathcal{I}m((f(\cdot, t), u_1(\cdot, t)) - g_1(t)\bar{u}_1(L, t)), \tag{4.4}$$

where we have used the fact that the potential V is real. By the Cauchy–Schwarz inequality, we get after integration in time

$$\begin{aligned} \|u_1(\cdot, t)\|^2 + p \int_0^t |u_1(L, s)|^2 ds &\leq \|u_0\|^2 + \int_0^t \|f(\cdot, s)\|^2 ds + \frac{1}{p} \int_0^t |g_1(s)|^2 ds \\ &\quad + \int_0^t \|u_1(\cdot, s)\|^2 ds. \end{aligned}$$

Applying the Grönwall Lemma gives the first bounds for u_1 :

$$\begin{aligned} & \|u_1\|_{L^\infty(0,T;L^2(\Omega_1))}^2 + p\|u_1(L, \cdot)\|_{L^2(0,T)}^2 \\ & \leq e^T \left(\|u_0\|^2 + \|f\|_{L^2(0,T;L^2(\Omega_1))}^2 + \frac{1}{p} \|g_1\|_{L^2(0,T)}^2 \right). \end{aligned} \tag{4.5}$$

We apply (4.5) to $\partial_t u_1$, with the initial condition $\partial_t u_1(\cdot, 0) = -i(f(\cdot, 0) - \partial_{xx} u_0 + Vu_0)$ in $L^2(\Omega_1)$. By the regularity assumptions on the data, and the Trace Theorem in time for f , we obtain

$$\begin{aligned} & \|\partial_t u_1\|_{L^\infty(0,T;L^2(\Omega_1))}^2 + \|\partial_t u_1(L, \cdot)\|_{L^2(0,T)}^2 \\ & \leq Ce^T \left(\|u_0\|_{H^2(\Omega_1)}^2 + \|V\|_{L^\infty(\Omega_1)}^2 \|u_0\|_{L^2(\Omega_1)}^2 \right. \\ & \quad \left. + \|f\|_{H^1(0,T;L^2(\Omega_1))}^2 + \frac{1}{p} \|g_1\|_{H^1(0,T)}^2 \right). \end{aligned} \tag{4.6}$$

(ii) Second *a priori* estimates. We now multiply the equation by $\partial_t \bar{u}_1$, integrate by parts in space, using the boundary condition, and take the real part. We obtain

$$\begin{aligned} & -\frac{d}{dt} \|\partial_x u_1\|^2 + 2p \operatorname{Re}(iu_1(L, \cdot) \partial_t \bar{u}_1(L, \cdot)) \\ & = -2 \operatorname{Re}(g_1 \partial_t \bar{u}_1(L, \cdot)) + 2 \operatorname{Re}(Vu_1(\cdot, t), \partial_t \bar{u}_1(\cdot, t)) \\ & \quad + 2 \operatorname{Re}(f(\cdot, t), \partial_t \bar{u}_1(\cdot, t)), \end{aligned}$$

which implies

$$\begin{aligned} \|\partial_x u_1(\cdot, t)\|^2 & \leq p\|u_1(L, \cdot)\|_{L^2(0,T)}^2 + (p + 1)\|\partial_t u_1(L, \cdot)\|_{L^2(0,T)}^2 \\ & \quad + 2\|\partial_t u_1\|_{L^2((0,T)\times\Omega_1)}^2 + \|V\|_{L^\infty(\Omega_1)}^2 \|u_1\|_{L^2((0,T)\times\Omega_1)}^2 \\ & \quad + \|f\|_{L^2((0,T)\times\Omega_1)}^2 + \|g_1\|_{L^2(0,T)}^2 + \|\partial_x u_0\|^2, \end{aligned}$$

and by (4.5), (4.6),

$$\begin{aligned} \|\partial_x u_1(\cdot, t)\|_{L^\infty(0,T;L^2(\Omega_1))}^2 & \leq Ce^T (\|u_0\|_{H^2(\Omega_1)}^2 + \|V\|_{L^\infty(\Omega_1)}^2 \|u_0\|_{L^2(\Omega_1)}^2 \\ & \quad + \|f\|_{H^1(0,T;L^2(\Omega_1))}^2 + \|g_1\|_{H^1(0,T)}^2). \end{aligned} \tag{4.7}$$

Finally, using the equation and (4.6), we have

$$\begin{aligned} \|\partial_{xx} u_1(\cdot, t)\|_{L^\infty(0,T;L^2(\Omega_1))}^2 & \leq Ce^T (\|u_0\|_{H^2(\Omega_1)}^2 + \|V\|_{L^\infty(\Omega_1)}^2 \|u_0\|_{L^2(\Omega_1)}^2 \\ & \quad + \|f\|_{H^1(0,T;L^2(\Omega_1))}^2 + \|g_1\|_{H^1(0,T)}^2). \end{aligned} \tag{4.8}$$

By (4.5)–(4.8), we have a bound on u_1 in $H^{2,1}(\Omega_1 \times (0, T))$, and on $u_1(L, \cdot)$ in $H^1(0, T)$. This is sufficient to obtain the existence and uniqueness in these spaces by the Galerkin method. Furthermore, by the Trace Theorem in $H^{2,1}(\Omega_1 \times (0, T))$, we have $u_1(0, \cdot)$ in $H^{3/4}(0, T)$.

(iii) Third *a priori* estimates. We assume now that $L > 0$ and that the potential V is constant. We prove that $u_1(0, \cdot)$ is actually in $H^1(0, T)$. With the additional

assumptions on the data, the solution u to (2.1), (2.2) is in $H^{4,2}(\Omega_1 \times (0, T))$.¹⁴ We introduce the auxiliary problem satisfied by $z = e^{-t}(u_1 - u)$ in $\Omega_1 \times (0, T)$:

$$\begin{cases} i\partial_t z + iz + \partial_{xx} z - Vz = 0 & \text{in } \Omega_1 \times (0, T), \\ z(\cdot, 0) = 0 & \text{in } \Omega_1, \\ \partial_x z(L, \cdot) = ipz(L, \cdot) + h & \text{in } (0, T), \end{cases} \tag{4.9}$$

with $h(t) = e^{-t}(g_1(t) - \mathcal{B}_1^r u(L, t))$. The boundary data h is in $H^1(0, T)$. Due to the compatibility conditions (4.2), we can extend h in $H^1(\mathbb{R})$ by H , vanishing for negative t , and we have through Fourier transform in time,

$$\hat{z}(x, \tau) = \frac{\hat{H}(\tau)}{(\tau + V - i)^{1/2} - ip} e^{-(\tau + V - i)^{1/2}(L - x)}, \quad x < L. \tag{4.10}$$

Since $\text{Im}(\tau + V - i)^{1/2} \leq 0$ and $p > 0$, we have $|\hat{z}(0, \tau)| \leq \frac{1}{p} |\hat{H}(\tau)|$, and

$$\|z(0, \cdot)\|_{H^1(0, T)} \leq \frac{1}{p} \|h\|_{H^1(0, T)},$$

which proves that $u_1(0, \cdot)$ is in $H^1(0, T)$, and

$$\|u_1(0, \cdot)\|_{H^1(0, T)}^2 \leq Ce^T (\|u\|_{H^{4,2}(\Omega_1 \times (0, T))}^2 + \|g_1\|_{H^1(0, T)}^2). \tag{4.11}$$

To conclude the proof of the proposition, we need to prove (4.3). Since u is in $H^{4,2}(\Omega_1 \times (0, T))$, it satisfies

$$\lim_{t \rightarrow 0_+} \mathcal{B}_2^r u(0, t) = \mathcal{B}_2^r u_0(0).$$

Therefore we only need to prove that

$$\lim_{t \rightarrow 0_+} \mathcal{B}_2^r z(0, t) = 0.$$

Since $h(0) = 0$, using the boundary condition, this amounts to proving that $\lim_{t \rightarrow 0_+} z(0, t) = 0$. Since H_1 is supported in \mathbb{R}_+ , \hat{H}_1 is analytic in the half-plane $\text{Im } \tau < 0$, and by (4.10) and Paley–Wiener Theorem,²⁰ $z(0, \cdot)$ is supported in \mathbb{R}_+ . Since we just proved that $z(0, \cdot)$ is in $H^1(0, T)$, and since $H^1(0, T) \subset C([0, T])$, by the Sobolev Embedding Theorem,¹⁴ we have $\lim_{t \rightarrow 0_+} z(0, t) = 0$. □

Remark 4.2. Let us explain why the results of Proposition 4.1 are weaker in the case $L > 0$. Indeed, the compatibility conditions (4.1) together with the energy estimates (4.5) and (4.6) imply that $u_1(L, \cdot)$ belongs to $H^1(0, T)$. This is sufficient to conclude in the case $L = 0$. In the case $L > 0$, we still have to prove that $u_1(0, \cdot)$ belongs to $H^1(0, T)$. Now, the interior trace $u_1(0, \cdot)$ is *a priori* less regular than the boundary data $u_1(L, \cdot)$ since it is only in $H^{3/4}(0, T)$ by the Trace Theorem in $H^{2,1}(\Omega_1 \times (0, T))$. To overcome this problem, we consider the case of a constant potential V in order to take advantage of explicit computations using the Fourier transform (see part (iii) of the proof of Proposition 4.1).

Theorem 4.1. *Let $L = 0$ and let V in $L^\infty(\mathbb{R})$. Let $p > 0$, and let g_L and g_0 be given in $H^1(0, T)$. Then algorithm (3.1) with Robin transmission operators (4.1) defines a sequence of iterates (u_1^k, u_2^k) in $H^{2,1}(\Omega_1 \times (0, T)) \times H^{2,1}(\Omega_2 \times (0, T))$, with $u_1^k(0, \cdot)$, $\partial_x u_1^k(0, \cdot)$, $u_2^k(L, \cdot)$ and $\partial_x u_2^k(L, \cdot)$ in $H^1(0, T)$.*

The same conclusion holds when $L > 0$ provided V is a real constant and g_L and g_0 satisfy the compatibility conditions

$$\partial_x u_0(L) - ipu_0(L) = g_L(0), \quad \partial_x u_0(0) + ipu_0(0) = g_0(0). \tag{4.12}$$

Proof. The proof is done by induction using Proposition 4.1. □

4.2. Convergence of the overlapping algorithm

Theorem 4.2. *Let V be a real constant. Let an initial guess (g_1, g_2) in $H^1(0, T)$, with the compatibility conditions (4.12). For $p > 0$, the solution (u_1^k, u_2^k) of algorithm (3.1) with complex Robin transmission conditions (4.1) converges in $L^2(\Omega_1 \times (0, T)) \times L^2(\Omega_2 \times (0, T))$ to the solution u in (2.1).*

Proof. We define the errors $e_j^k = u_j^k - u$, $j = 1, 2$, solving the homogeneous algorithm, and introduce the interface functions $h_j^k = \mathcal{B}_j^r e_j^k$. The proof uses Fourier analysis. Proceeding as in (4.9), we define the local convergence factor by

$$\theta(\tau, L) = -\frac{(\tau + V - i)^{1/2} + ip}{(\tau + V - i)^{1/2} - ip} e^{-(\tau + V - i)^{1/2} L} \tag{4.13}$$

and obtain

$$\mathcal{F}(e^{-t} h_1^k, e^{-t} h_2^k) = \theta(\tau, L) \mathcal{F}(e^{-t} h_2^{k-1}, e^{-t} h_1^{k-1}).$$

Thus

$$|\mathcal{F}(e^{-t} h_1^k, e^{-t} h_2^k)| = |\theta(\tau, L)|^k |\mathcal{F}(e^{-t} h_1, e^{-t} h_2)|.$$

Since $p > 0$, $|\theta(\tau, L)|$ is strictly smaller than 1 for all τ . Thus, Lebesgue convergence theorem immediately yields:

$$\lim_{k \rightarrow +\infty} \|(e^{-t} h_1^k, e^{-t} h_2^k)\|_{(H^1(0, T))^2} = 0. \tag{4.14}$$

Now, using formula (4.10), we obtain:

$$\mathcal{F}(e^{-t} e_1^k)(x, \tau) = \frac{\mathcal{F}(e^{-t} h_1^{k-1})(\tau)}{(\tau + V - i)^{1/2} - ip} e^{-(\tau + V - i)^{1/2}(L-x)}, \quad x < L. \tag{4.15}$$

Thus, we have:

$$\|\mathcal{F}(e^{-t} e_1^k)(\cdot, \tau)\|_{L^2(\Omega_1)}^2 = \frac{|\mathcal{F}(e^{-t} h_1^{k-1})(\tau)|^2}{2 \operatorname{Re}((\tau + V - i)^{1/2}) |(\tau + V - i)^{1/2} - ip|^2}. \tag{4.16}$$

Using (3.11) with $\eta = 1$, we deduce in each subdomain

$$\|e^{-t}e_j^k\|_{L^2(0,T;L^2(\Omega_j))} \leq \|e^{-t}h_j^{k-1}\|_{L^2(0,T)} \leq \|e^{-t}h_j^{k-1}\|_{H^1(0,T)},$$

which together with (4.14) yields:

$$\lim_{k \rightarrow +\infty} \|e_j^k\|_{L^2(\Omega_j \times (0,T))} = 0, \tag{4.17}$$

which completes the proof. □

Remark 4.3. The classical Schwarz algorithm has a convergence factor equal to $e^{-(\tau+V-i)^{1/2}L}$. Therefore the complex Robin algorithm converges at least as fast as the classical one. We will see that we can find p such as to minimize the convergence factor.

4.3. Convergence of the non-overlapping algorithm

We now assume that there is no overlap, i.e. $L = 0$. We first analyze the convergence of the algorithm in the appropriate Sobolev spaces. The proof, though much easier, follows the same path as in Sec. 3.2.

Theorem 4.3. *Without overlap, $L = 0$, the complex Robin–Schwarz waveform relaxation algorithm (3.1) with transmission conditions (4.1) converges for $p > 0$ in $L^\infty(0, T; L^2(\Omega_1)) \times L^\infty(0, T; L^2(\Omega_2))$ to the solution u in (2.1), (2.2) for any initial guess (g_1, g_2) in $(H^1(0, T))^2$ and any real potential V in $L^\infty(\mathbb{R})$.*

Proof. We use the energy estimate (4.4) in Ω_1 for the error e_1^k , and the corresponding energy estimate in Ω_2 for the error e_2^k ,

$$\frac{1}{2} \frac{d}{dt} \|e_1^k\|^2 + \mathcal{I}m(\partial_x e_1^k(0) \overline{e_1^k(0)}) = 0, \quad \frac{1}{2} \frac{d}{dt} \|e_2^k\|^2 - \mathcal{I}m(\partial_x e_2^k(0) \overline{e_2^k(0)}) = 0.$$

We rewrite the terms on the interface in the form $\mathcal{I}m(\partial_x e_j(0, \cdot) \overline{e_j(0, \cdot)}) = \frac{1}{4p} (|\mathcal{B}_i^r e_j(0, \cdot)|^2 - |\mathcal{B}_j^r e_i(0, \cdot)|^2)$, for $j \neq i$, and we obtain the new energy estimates

$$\frac{d}{dt} \|e_i^k\|^2 + \frac{1}{2p} |\mathcal{B}_j^r e_i^k(0, \cdot)|^2 = \frac{1}{2p} |\mathcal{B}_i^r e_i^k(0, \cdot)|^2.$$

Replacing the transmission conditions, we find

$$\frac{d}{dt} \|e_i^k\|^2 + \frac{1}{2p} |\mathcal{B}_j^r e_i^k(0, \cdot)|^2 = \frac{1}{2p} |\mathcal{B}_i^r e_j^{k-1}(0, \cdot)|^2, \quad (i, j) = (1, 2) \text{ or } (2, 1).$$

Adding the equations in Ω_1 and Ω_2 , and summing in k , we get finally

$$\begin{aligned} & \sum_{k=1}^K \frac{d}{dt} (\|e_1^k\|^2 + \|e_2^k\|^2) + \frac{1}{2p} (|\mathcal{B}_2^r e_1^K|^2 + |\mathcal{B}_1^r e_2^K|^2)(0, \cdot) \\ & = \frac{1}{2p} (|\mathcal{B}_2^r e_1^0|^2 + |\mathcal{B}_1^r e_2^0|^2)(0, \cdot). \end{aligned} \tag{4.18}$$

We can now integrate in time, and since the initial values of the error vanish, the sum of the energies over all the iterates remains bounded. Hence the energy in the iterates needs to go to zero and the algorithm converges. \square

4.4. Optimization of the algorithm with overlap

We suppose here the potential to be constant. The errors are given recursively by

$$\mathcal{F}e_j^{k+1} = \rho(\cdot, p, L)\mathcal{F}e_l^k \quad \text{on } \Gamma_j \times (0, T), \quad j \neq l,$$

where $\rho(\tau, p, L)$ is the convergence factor associated with complex Robin transmission conditions,

$$\rho(\tau, p, L) = \frac{ip + (\tau + V)^{1/2}}{ip - (\tau + V)^{1/2}} e^{-(\tau+V)^{1/2}L}. \tag{4.19}$$

The smaller the convergence factor, the faster the algorithm. In practical computations, only a bounded range of frequencies are present: $|\tau| \in [\tau_{\min}, \tau_{\max}]$. For a discretization with time-step Δt , we have $\tau_{\max} = \pi/\Delta t$, $\tau_{\min} = \pi/T$. We define $D = (-\tau_{\max}, -\tau_{\min}) \cup (\tau_{\min}, \tau_{\max})$, and for a given potential V , the evanescent region $E_V = \{\tau \in D, \tau > V\}$, and the propagating region $P_V = \{\tau \in D, \tau < V\}$. The modulus of the convergence factor is given by:

$$|\rho(\tau, p, L)| = \begin{cases} e^{-\sqrt{\tau+V}L} & \tau \in E_V, \\ \left| \frac{p - \sqrt{\tau + V}}{p + \sqrt{\tau + V}} \right| & \tau \in P_V. \end{cases} \tag{4.20}$$

The overlap provides an exponential decay of the convergence factor in the evanescent regime, whereas the parameter p is meant to accelerate the convergence in the propagating regime. Notice that without overlap, the evanescent modes are not damped, even if the algorithm converges (see Fig. 5).

The following min–max problem is the key of the minimization in P_V . We introduce the function

$$f(s, p) = \left| \frac{p - s}{p + s} \right|, \tag{4.21}$$

and the best approximation problem: find $p^* > 0$ such as to realize

$$\inf_{p>0} \sup_{s \in (s_{\min}, s_{\max})} f(s, p). \tag{4.22}$$

Problem (4.22) is quite simple and can be treated at hand.

Lemma 4.1. *The best approximation problem (4.22) has a unique solution p^* , defined by $f(s_{\min}, p^*) = f(s_{\max}, p^*)$, and given by*

$$p^* = (s_{\min} s_{\max})^{1/2}, \quad s^* = s_{\min}, \quad f^* = f(s^*, p^*) = \frac{\sqrt{s_{\max}} - \sqrt{s_{\min}}}{\sqrt{s_{\max}} + \sqrt{s_{\min}}}.$$

Proof. It is easy to see that for any positive p ,

$$\sup_{s \in (s_{\min}, s_{\max})} \left| \frac{p-s}{p+s} \right| = \begin{cases} \left| \frac{s_{\max}-p}{s_{\max}+p} \right| & \text{if } p \leq \sqrt{s_{\max}s_{\min}}, \\ \left| \frac{p-s_{\min}}{p+s_{\min}} \right| & \text{if } p \geq \sqrt{s_{\max}s_{\min}}. \end{cases}$$

The function $p \mapsto \sup_{s \in [s_{\min}, s_{\max}]} \left| \frac{p-s}{p+s} \right|$ is decreasing on $(0, \sqrt{s_{\max}s_{\min}})$ and increasing on $(\sqrt{s_{\max}s_{\min}}, +\infty)$. It has a unique minimum, attained for $p^* = \sqrt{s_{\max}s_{\min}}$. \square

It is now very easy to find the optimal coefficient p , and the technical details can be found in Halpern–Szeftel.¹²

5. Construction of the Discrete Algorithms

The discretization parameters are Δx and Δt in space and time respectively, the discrete points in space are denoted by $x_j = j\Delta x$, and in time $t^n = n\Delta t$, with $\Delta t = T/N$. The discrete difference operators are defined by

$$\begin{aligned} D_x^+ U(j, n) &= \frac{U(j+1, n) - U(j, n)}{\Delta x}, & D_x^- U(j, n) &= \frac{U(j, n) - U(j-1, n)}{\Delta x}, \\ D_t^+ U(j, n) &= \frac{U(j, n+1) - U(j, n)}{\Delta t}, & F\left(n + \frac{1}{2}\right) &= \frac{1}{2}(F(n) + F(n+1)). \end{aligned} \tag{5.1}$$

We use the Crank–Nicolson scheme for the discretization of the equation in the interior.

$$\begin{aligned} LU(j, n) &= iD_t^+ U(j, n) + D_x^+ D_x^- U\left(j, n + \frac{1}{2}\right) - V(j)U\left(j, n + \frac{1}{2}\right) \\ &= F\left(j, n + \frac{1}{2}\right), \end{aligned} \tag{5.2}$$

which is unconditionally stable, second order in time and space. We assume that $L = \ell\Delta x$. The points in Ω_1 are numbered from $-\infty$ to ℓ , and the points in Ω_2 are numbered from 0 to $+\infty$. We denote the numerical approximation to $u_i^k(j\Delta x, n\Delta t)$ in Ω_i at iteration step k by $U_i^k(j, n)$. The discrete form of algorithm (3.1) is given by an initial guess (G_1^0, G_2^0) and, for $k \geq 1$,

$$\begin{cases} LU_1^k(j, n) = F\left(j, n + \frac{1}{2}\right) & \text{for } -\infty < j < \ell, \quad 0 \leq n \leq N, \\ U_1^k(j, 0) = u_0(x_j) & \text{for } -\infty < j \leq \ell, \\ B_1 U_1^k(\ell, n) = G_1^{k-1}(n) - \frac{\Delta x}{2} F\left(\ell, n + \frac{1}{2}\right) & \text{for } 0 \leq n \leq N, \end{cases} \tag{5.3}$$

$$\begin{cases} LU_2^k(j, n) = F\left(j, n + \frac{1}{2}\right) & \text{for } 0 < j < +\infty, \quad 0 \leq n \leq N, \\ U_2^k(j, 0) = u_0(x_j) & \text{for } 0 \leq j < +\infty, \\ B_2U_2^k(0, n) = G_0^{k-1}(n) + \frac{\Delta x}{2}F\left(0, n + \frac{1}{2}\right) & \text{for } 0 \leq n \leq N. \end{cases} \tag{5.4}$$

The new values on the boundaries are:

$$\begin{cases} G_1^k(n) = \tilde{B}_1U_2^k(\ell, n) - \frac{\Delta x}{2}F\left(\ell, n + \frac{1}{2}\right) & \text{for } 0 \leq n \leq N, \\ G_2^k(n) = \tilde{B}_2U_1^k(0, n) + \frac{\Delta x}{2}F\left(0, n + \frac{1}{2}\right) & \text{for } 0 \leq n \leq N. \end{cases} \tag{5.5}$$

5.1. The complex Robin discrete algorithm

For complex Robin transmission conditions, the discrete transmission operators B_j^r and \tilde{B}_j^r are given below

$$\begin{aligned} B_1^rU_1(\ell, n) &= D_x^-U_1\left(\ell, n + \frac{1}{2}\right) - ipU_1\left(\ell, n + \frac{1}{2}\right) \\ &\quad - i\frac{\Delta x}{2}D_t^+U_1(\ell, n) - \frac{\Delta x}{2}V(\ell)U_1\left(\ell, n + \frac{1}{2}\right), \\ B_2^rU_2(0, n) &= D_x^+U_2\left(0, n + \frac{1}{2}\right) + ipU_2\left(0, n + \frac{1}{2}\right) \\ &\quad + i\frac{\Delta x}{2}D_t^+U_2(0, n) + \frac{\Delta x}{2}V(0)U_2\left(0, n + \frac{1}{2}\right), \\ \tilde{B}_2^rU_1(0, n) &= D_x^-U_1\left(0, n + \frac{1}{2}\right) + ipU_1\left(0, n + \frac{1}{2}\right) \\ &\quad - i\frac{\Delta x}{2}D_t^+U_1(0, n) - \frac{\Delta x}{2}V(0)U_1\left(0, n + \frac{1}{2}\right), \\ \tilde{B}_1^rU_2(\ell, n) &= D_x^+U_2\left(\ell, n + \frac{1}{2}\right) - ipU_2\left(\ell, n + \frac{1}{2}\right) \\ &\quad + i\frac{\Delta x}{2}D_t^+U_2(\ell, n) + \frac{\Delta x}{2}V(\ell)U_2\left(\ell, n + \frac{1}{2}\right). \end{aligned} \tag{5.6}$$

The previous formulas are useful for the practical implementation of the algorithm. In the forthcoming convergence analysis, we shall use the transmission conditions in the form

$$\begin{aligned} B_1^rU_1^k(\ell, n) &= \tilde{B}_1^rU_2^{k-1}(\ell, n) - \Delta xF\left(\ell, n + \frac{1}{2}\right), \\ B_2^rU_2^k(0, n) &= \tilde{B}_2^rU_1^{k-1}(0, n) + \Delta xF\left(0, n + \frac{1}{2}\right). \end{aligned} \tag{5.7}$$

The above boundary operators are obtained using a finite volume procedure which is given in details in Halpern–Szeftel.¹² This idea was first introduced in Gander *et al.*¹⁰ for the wave equation in one dimension.

5.2. The quasi-optimal discrete algorithm

Arnold and Ehrhardt² designed discrete transparent boundary condition for the Crank–Nicolson scheme, in the case of a constant potential outside the domain. They use the operators

$$B_1^{qo}U(\ell, n) = U(\ell - 1, n + 1) + U(\ell - 1, n) - \sum_{m=1}^{n+1} S_\ell(n - m + 1)U(\ell, m), \tag{5.8}$$

$$B_2^{qo}U(0, n) = U(1, n + 1) + U(1, n) - \sum_{m=1}^{n+1} S_0(n - m + 1)U(0, m), \tag{5.9}$$

where the coefficients $S_j(m)$ are defined in the following formulas:

$$\begin{aligned} R &= 2 \frac{\Delta x^2}{\Delta t}, \quad \sigma_j = V(x_j)\Delta x^2, \\ \alpha_j &= \frac{i}{2} e^{i\phi_j/2} ((R^2 + \sigma_j^2)(R^2 + (\sigma_j + 4)^2))^{1/4}, \\ \mu_j &= \frac{(R^2 + 4\sigma_j + \sigma_j^2)}{((R^2 + \sigma_j^2)(R^2 + (\sigma_j + 4)^2))^{1/2}}, \\ \phi_j &= \arctan \left(2R \frac{\sigma_j + 2}{R^2 - 4\sigma_j - \sigma_j^2} \right), \\ S_j(0) &= 1 - \frac{iR}{2} + \frac{\sigma_j}{2} - \alpha_j, \\ S_j(1) &= 1 + \frac{iR}{2} + \frac{\sigma_j}{2} + \alpha_j \mu_j e^{-i\phi_j}, \\ S_j(2) &= \frac{\alpha_j}{2} e^{-2i\phi_j} (\mu_j^2 - 1), \\ S_j(m + 2) &= \frac{2m - 1}{m + 1} \mu_j e^{-i\phi_j} S_j(m + 1) - \frac{m - 2}{m + 1} e^{-2i\phi_j} S_j(m), \quad m \geq 1. \end{aligned} \tag{5.10}$$

Using these transparent boundary operators as transmission operator in the domain decomposition process, we write, for $k \geq 1$, and $1 \leq n \leq N$,

$$B_1^{qo}U_1^k(\ell, n) = G_1^{k-1}(n), \quad B_2^{qo}U_2^k(0, n) = G_2^{k-1}(n), \tag{5.11}$$

and define, for $1 \leq n \leq N$,

$$\begin{aligned}
 G_1^k(n) &= 4U_2^k\left(\ell, n + \frac{1}{2}\right) - 2U_2^k\left(\ell + 1, n + \frac{1}{2}\right) \\
 &\quad - \sum_{m=1}^{n+1} S_\ell(n - m + 1)U_2^k(\ell, m) \\
 &\quad - 2i \frac{\Delta x^2}{\Delta t} (U_2^k(\ell, n + 1) - U_2^k(\ell, n)) \\
 &\quad - 2\Delta x^2 V(\ell)U_2^k\left(\ell, n + \frac{1}{2}\right) + 2\Delta x^2 F\left(\ell, n + \frac{1}{2}\right), \\
 G_2^k(n) &= 4U_1^k\left(0, n + \frac{1}{2}\right) - 2U_1^k\left(-1, n + \frac{1}{2}\right) \\
 &\quad - \sum_{m=1}^{n+1} S_0(n - m + 1)U_1^k(0, m) \\
 &\quad - 2i \frac{\Delta x^2}{\Delta t} (U_1^k(0, n + 1) - U_1^k(0, n)) \\
 &\quad - 2\Delta x^2 V(0)U_1^k\left(0, n + \frac{1}{2}\right) + 2\Delta x^2 F\left(0, n + \frac{1}{2}\right).
 \end{aligned} \tag{5.12}$$

Here, we do not find G_1^k and G_2^k through a finite volume procedure. Instead, we simply choose them such that we obtain the Crank–Nicolson scheme (5.2) when $U = U_1 = U_2$, i.e. after the domain decomposition method has converged.

Remark 5.1. Other choices of discrete transparent boundary conditions could be used to discretize the quasi-optimal algorithm.¹

6. Convergence of the Discrete Complex Robin Algorithm

For the overlapping algorithm, the convergence will be obtained by a normal mode analysis, whereas energy estimates will prove the convergence in the non-overlapping case. We start by studying the discrete Crank–Nicolson scheme.

6.1. The Crank–Nicolson scheme

In this section, V is a real constant. We introduce the normal mode analysis.²² The discrete Laplace transform of a grid function $w = \{w_n\}_{n \geq 0}$ on a regular grid with time step Δt is defined for $\eta > 0$ by

$$\mathcal{L}w(s) = \widehat{w}(s) = \frac{1}{\sqrt{2\pi}} \Delta t \sum_{n \geq 0} e^{-sn\Delta t} w_n, \quad s = \eta + i\tau, \quad |\tau| \leq \frac{\pi}{\Delta t}, \tag{6.1}$$

and the inversion formula is given by

$$w_n = \frac{1}{\sqrt{2\pi}} \int_{-\frac{\pi}{\Delta t}}^{\frac{\pi}{\Delta t}} e^{sn\Delta t} \widehat{w}(s) d\tau = -\frac{i}{\sqrt{2\pi}} \int_{|z|=e^{\eta\Delta t}} z^{n-1} \widehat{w}(z) dz.$$

The corresponding norms are

$$\|w\|_{\eta, \Delta t} = \left(\Delta t \sum_{n \geq 0} e^{-2\eta n \Delta t} |w_n|^2 \right)^{\frac{1}{2}}, \quad \|\widehat{w}\|_{\eta} = \left(\int_{-\frac{\pi}{\Delta t}}^{\frac{\pi}{\Delta t}} |\widehat{w}(\eta + i\tau)|^2 d\tau \right)^{\frac{1}{2}}, \tag{6.2}$$

and we have Parseval's equality

$$\|w\|_{\eta, \Delta t} = \|\widehat{w}\|_{\eta}. \tag{6.3}$$

Suppose now $W(j, n)$ to be a solution to the difference equation

$$iD_t^+ W(j, n) + D_x^+ D_x^- W\left(j, n + \frac{1}{2}\right) - VW\left(j, n + \frac{1}{2}\right) = 0, \tag{6.4}$$

with initial condition $W(j, 0) = 0$. We denote by $\widehat{W}(j, s)$ the discrete Laplace transform in time of $W(j, n)$. Equation (6.4) becomes the difference equation in one variable, s acting as a parameter

$$\widehat{W}(j - 1, s) + 2(i\gamma h(z) - 1 - \Delta x^2 V) \widehat{W}(j, s) + \widehat{W}(j + 1, s) = 0, \tag{6.5}$$

with $z = e^{s\Delta t}$, $h(z) = \frac{z-1}{z+1}$ and $\gamma = \Delta x^2 / \Delta t$. Function h is a well-known homographic transformation, whose properties we summarize now:

- Lemma 6.1.** (1) *The function h maps the circle of center O and radius 1 onto the line $\operatorname{Re} Z = 0$.*
 (2) *The function h maps the exterior of the closed disk of center O and radius 1 onto the half-plane $\operatorname{Re} Z > 0$.*
 (3) *The function h maps any circle of center O and radius $a > 1$ onto the circle of center $(a^2 + 1)/(a^2 - 1)$ and radius $2a/(a^2 - 1)$.*

We introduce the characteristic second-order equation

$$r^2 + 2(i\gamma h(z) - 1 - \Delta x^2 V)r + 1 = 0. \tag{6.6}$$

The roots of (6.6) satisfy

$$r_+ r_- = 1, \quad r_+ + r_- = 2(1 + \Delta x^2 V - i\gamma h(z)). \tag{6.7}$$

Lemma 6.2. *For $|z| > 1$ (i.e. $\eta > 0$), Eq. (6.6) has two distinct roots r_{\pm} with $|r_-| < 1 < |r_+|$. Furthermore, these roots are not real.*

Proof. Suppose $|z| > 1$. By (6.7), the first assertion in the lemma holds true, unless $|r_-| = |r_+| = 1$. In that case we have $r_- = \bar{r}_+$, and therefore $r_+ + r_-$ is real, which implies by (6.7) that $h(z)$ is pure imaginary. This last assertion is equivalent by Lemma 6.1 to $|z| = 1$, hence the contradiction. \square

6.2. The overlapping complex Robin Schwarz relaxation algorithm

Now we consider algorithm (5.3)–(5.5) with transmission conditions (5.7). If U is the solution to the Crank–Nicolson scheme in $\mathbb{N} \times \{0, \dots, N\}$, it satisfies $B_1^r U(\ell, n) = \tilde{B}_1^r U(\ell, n) - \Delta x F(\ell, n + \frac{1}{2})$, and $B_2^r U(0, n) = \tilde{B}_2^r U(0, n) + \Delta x F(0, n + \frac{1}{2})$. Therefore the errors satisfy the algorithm with vanishing data, and we can use the results of Sec. 6.1. We deduce from Lemma 6.2 that for $\eta > 0$, any solution to (6.5) is a linear combination of the powers of r_+ and r_- , and there exist functions $a_i^k(s)$ such that

$$\widehat{W}_1^k(j, s) = a_1^k(s)r_+^{j-\ell}, \quad j \leq \ell, \quad \widehat{W}_2^k(j, s) = a_2(s)r_-^j, \quad j \geq 0. \tag{6.8}$$

The transmission conditions in (5.7) impose

$$a_1^k(s) = R_R(z, \gamma, p, \ell)a_2^{k-1}(s), \quad a_2^k(s) = R_R(z, \gamma, p, \ell)a_1^{k-1}(s), \quad \text{with}$$

$$R_R(z, \gamma, p, \ell) = -r_-^\ell \frac{1 + \Delta x^2 V - r_- - i\gamma h(z) + ip\Delta x}{1 + \Delta x^2 V - r_- - i\gamma h(z) - ip\Delta x}. \tag{6.9}$$

Lemma 6.3. *For any s with $\eta = \operatorname{Re} s > 0$, for any $p > 0$, for any $\ell \geq 0$, the discrete convergence factor for the complex Robin transmission conditions satisfies*

$$|R_R(z, \gamma, p, \ell)| < |r_-|^\ell \leq 1.$$

Proof. We define

$$\alpha(z, \gamma, p) = \frac{1 + \Delta x^2 V - r_- - i\gamma h(z) + ip\Delta x}{1 + \Delta x^2 V - r_- - i\gamma h(z) - ip\Delta x}.$$

The modulus of $\alpha(z, \gamma, p)$ is given by:

$$|\alpha(z, \gamma, p)| = \sqrt{\frac{(1 + \Delta x^2 V - \operatorname{Re}(r_-) + \gamma \operatorname{Im}(h(z)))^2 + (-\operatorname{Im}(r_-) - \gamma \operatorname{Re}(h(z)) + p\Delta x)^2}{(1 + \Delta x^2 V - \operatorname{Re}(r_-) + \gamma \operatorname{Im}(h(z)))^2 + (\operatorname{Im}(r_-) + \gamma \operatorname{Re}(h(z)) + p\Delta x)^2}}.$$

Since $\operatorname{Re} h(z) = \frac{|z|^2 - 1}{|z + 1|^2}$ and $|z| > 1$, we have $\operatorname{Re} h(z) > 0$. Also, by Lemma 6.2 and (6.7), we compute

$$\operatorname{Im}(r_-) = \frac{2\gamma \operatorname{Re}(h(z))}{|r_+|^2 - 1},$$

which yields $\operatorname{Im}(r_-) > 0$. Therefore $|\alpha(z, \gamma, p)| < 1$ for any strictly positive p . Since $\|R_R\| = |\alpha||r_-|^\ell$, and $|r_-| \leq 1$ by Lemma 6.2, the lemma follows. \square

The interested reader can find a proof of the following result in Halpern–Szeftel¹²:

Theorem 6.1. *Let V be a real constant. Let U_p^k be the iterates of algorithm (5.3)–(5.5). For positive $p, \eta\Delta t$ sufficiently small but nonzero, and Δx sufficiently small, we have*

$$\|U_p^k - U\|_{\Omega_i, \eta, \Delta t} \lesssim (1 - \ell\eta\Delta x^2/2)^{k-1} \max_{p=1,2} \|U_p^1\|_{\Omega_p, \eta, \Delta t}.$$

6.3. The non-overlapping complex Robin Schwarz relaxation algorithm

We consider now the case where $\ell = 0$. For the complex Robin Schwarz relaxation algorithm, the convergence factor is $\alpha(z, \gamma, p)$. For $\eta > 0$ and $p > 0$, we have proved that $|\alpha(z, \gamma, p)| < 1$. This shows the convergence of the non-overlapping complex Robin Schwarz relaxation algorithm when V is a real constant.

However, our numerical computations are implemented with non-constant potentials. Thus, we introduce a proof of convergence based on energy estimates. It is the discrete analog to the proof of Theorem 4.3. The errors W_j^k are solutions for $k \geq 1$ to Eq. (5.2) with $F \equiv 0$ and vanishing initial values. The transmission conditions are for $k \geq 2$:

$$B_1 W_1^k(0, n) = \tilde{B}_1 W_2^{k-1}(0, n), \quad B_2 W_2^k(0, n) = \tilde{B}_2 W_1^{k-1}(0, n) \quad \text{for } 0 \leq n \leq N, \tag{6.10}$$

where the discrete transmission operators B_j and \tilde{B}_j are summarized in (5.6). The algorithm is initialized on the boundary, for $0 \leq n \leq N$, by

$$B_1 W_1^1(0, n) = \frac{\Delta x}{2} \tilde{G}_1(n) = \frac{\Delta x}{2} G_1(n) - \left(B_1 U(0, n) + \Delta x F\left(0, n + \frac{1}{2}\right) \right),$$

$$B_2 W_2^1(n) = \frac{\Delta x}{2} \tilde{G}_2(n) = \frac{\Delta x}{2} G_2(n) - \left(B_2 U(0, n) - \Delta x F\left(0, n + \frac{1}{2}\right) \right).$$

Theorem 6.2. *The discrete non-overlapping Schwarz waveform relaxation algorithm (5.3)–(5.5) converges for $p > 0$, in $l^\infty(0, N; l^2(-\infty, 0)) \times l^\infty(0, N; l^2(0, +\infty))$, to the solution U to (5.2), for any initial guess (G_0, G_L) and any positive p :*

$$\forall n, 0 \leq n \leq N, \quad \lim_{k \rightarrow +\infty} \Delta x \left[\sum'_{j \leq 0} |(W_1^k - U)(j, n)|^2 + \sum'_{j \geq 0} |(W_2^k - U)(j, n)|^2 \right] = 0 \tag{6.11}$$

with the usual notation $\sum'_{j \leq 0} W_j = W_0/2 + \sum_{j \leq -1} W_j$ and $\sum'_{j \geq 0} W_j = W_0/2 + \sum_{j \geq 1} W_j$.

Proof. We write energy estimates, using a discrete analogous to (2.3). We start with the left subdomain. We multiply Eq. (5.2) in Ω_1 by $W_1^k(j, n + \frac{1}{2})$, take the imaginary part, and sum for $j \leq -1$. The third term vanishes due to the fact that V is real-valued. The first term becomes

$$\frac{1}{2\Delta t} \sum_{j \leq -1} (|W_1^k(j, n + 1)|^2 - |W_1^k(j, n)|^2).$$

As for the second term, we perform a discrete integration by parts:

$$\begin{aligned} & \sum_{j \leq -1} \overline{W_1^k \left(j, n + \frac{1}{2} \right)} D_x^+ D_x^- W_1^k \left(j, n + \frac{1}{2} \right) \\ &= - \sum_{j \leq 0} \left| D_x^- W_1^k \left(j, n + \frac{1}{2} \right) \right|^2 + \frac{1}{\Delta x} \overline{W_1^k \left(0, n + \frac{1}{2} \right)} D_x^- W_1^k \left(0, n + \frac{1}{2} \right). \end{aligned}$$

Thus we can write

$$\begin{aligned} & \frac{1}{2\Delta t} \sum_{j \leq -1} (|W_1^k(j, n + 1)|^2 - |W_1^k(j, n)|^2) \\ & \quad + \frac{1}{\Delta x} \mathcal{I}m \overline{W_1^k \left(0, n + \frac{1}{2} \right)} D_x^- W_1^k \left(0, n + \frac{1}{2} \right) = 0, \end{aligned}$$

which we rewrite as

$$\begin{aligned} & \frac{1}{2\Delta t} \sum'_{j \leq 0} (|W_1^k(j, n + 1)|^2 - |W_1^k(j, n)|^2) \\ & \quad + \frac{1}{\Delta x} \mathcal{I}m \left[\overline{W_1^k \left(0, n + \frac{1}{2} \right)} \left(D_x^- W_1^k \left(0, n + \frac{1}{2} \right) - i \frac{\Delta x}{2} D_t^+ W_1^k(0, n) \right) \right] = 0. \end{aligned}$$

We now introduce the operators B_j defined in (5.6). We obtain:

$$\begin{aligned} & \frac{1}{2\Delta t} \sum'_{j \leq 0} (|W_1^k(j, n + 1)|^2 - |W_1^k(j, n)|^2) + \frac{1}{4p\Delta x} |\tilde{B}_2 W_1^k(0, n)|^2 \\ &= \frac{1}{4p\Delta x} |B_1 W_1^k(0, n)|^2. \end{aligned} \tag{6.12}$$

We obtain in the same way the estimates on the right:

$$\begin{aligned} & \frac{1}{2\Delta t} \sum'_{j \geq 0} (|W_2^k(j, n + 1)|^2 - |W_2^k(j, n)|^2) + \frac{1}{4p\Delta x} |\tilde{B}_1 W_2^k(0, n)|^2 \\ &= \frac{1}{4p\Delta x} |B_2 W_2^k(0, n)|^2. \end{aligned} \tag{6.13}$$

We now add (6.12) to (6.13), use the transmission conditions (6.10) for $k \geq 2$:

$$\begin{aligned} & \frac{1}{2\Delta t} \sum'_{j \leq 0} (|W_1^k(j, n + 1)|^2 - |W_1^k(j, n)|^2) \\ & \quad + \frac{1}{2\Delta t} \sum'_{j \geq 0} (|W_2^k(j, n + 1)|^2 - |W_2^k(j, n)|^2) \\ & \quad + \frac{1}{4p\Delta x} (|\tilde{B}_1 W_2^k(0, n)|^2 + |\tilde{B}_2 W_1^k(0, n)|^2) \\ &= \frac{1}{4p\Delta x} (|\tilde{B}_1 W_1^{k-1}(0, n)|^2 + |\tilde{B}_2 W_2^{k-1}(0, n)|^2). \end{aligned} \tag{6.14}$$

We now sum in time, for $0 \leq n \leq q - 1$:

$$\begin{aligned} & \frac{1}{2\Delta t} \left(\sum'_{j \leq 0} |W_1^k(j, q)|^2 + \sum'_{j \geq 0} |W_2^k(j, q)|^2 \right) \\ & \quad + \frac{1}{4p\Delta x} \sum_{n=1}^q (|\tilde{B}_2 W_1^k(0, n)|^2 + |\tilde{B}_1 W_2^k(0, n)|^2) \\ & = \frac{1}{4p\Delta x} \sum_{n=1}^q (|\tilde{B}_2 W_1^{k-1}(0, n)|^2 + |\tilde{B}_1 W_2^{k-1}(0, n)|^2). \end{aligned} \tag{6.15}$$

We finally sum (6.15) in k , for $1 \leq k \leq K$, multiply by $2\Delta t\Delta x$, and use the boundary values for the initial guess:

$$\begin{aligned} & \Delta x \sum_{k=2}^K \left(\sum'_{j \leq 0} |W_1^k(j, q)|^2 + \sum'_{j \geq 0} |W_2^k(j, q)|^2 \right) \\ & \quad + \frac{\Delta t}{2p} \sum_{n=1}^q (|\tilde{B}_2 W_1^K(0, n)|^2 + |\tilde{B}_1 W_2^K(0, n)|^2) \\ & = \frac{\Delta t}{2p} \sum_{n=1}^q \left(\left| \frac{\Delta x}{2} \tilde{G}_1(n) + 2ipW_1^1(0, n) \right|^2 \right. \\ & \quad \left. + \left| \frac{\Delta x}{2} \tilde{G}_2(n) - 2ipW_2^1(0, n) \right|^2 \right). \end{aligned} \tag{6.16}$$

The sum of the discrete L^2 norm over all iterates remains bounded. Thus:

$$\lim_{k \rightarrow +\infty} \Delta x \left(\sum'_{j \leq 0} |W_1^k(j, q)|^2 + \sum'_{j \geq 0} |W_2^k(j, q)|^2 \right) = 0. \tag{6.17}$$

□

7. Numerical Results

We study the actual efficiency of the algorithms: rate of convergence, robustness with respect to the length of the time interval, and to the mesh size.

In Sec. 7.1, we treat the free Schrödinger equation. We first show briefly the behavior of the classical Schwarz algorithm on the computation of a Gaussian traveling wave. Thereafter, and for the rest of the numerical analysis, we consider zero initial value, which is sufficient since the equation is linear. A random initial guess is used, in order to make sure that all frequencies are present in the analysis. We compare the classical and the complex Robin algorithms in case of two subdomains. We also study the efficiency of the complex Robin, as a function of the parameter p , in the overlapping and non-overlapping cases.

Then we turn to non-constant potential, like the potential barrier and perform a similar analysis.

In Sec. 7.3, we introduce the quasi-optimal algorithm.

Finally we explore in Sec. 7.4 the extension to several subdomains.

The physical domain is $(a, b) = (-5, +5)$. It is divided into two subdomains of equal size. Since no parallelism is involved yet, our algorithms are implemented the alternate way, i.e. we compute U_1 with g_1 , then deduce g_2 and transmit it to the right domain for the computation of U_2 . Thus iteration $\#k$ in this section corresponds to the computation of U_1^{2k-1}, U_2^{2k} in the previous setting.

7.1. The free Schrödinger equation

We first study the properties of the classical Schwarz algorithm with Dirichlet transmission conditions, then those of the complex Robin algorithm, and compare their efficiency. We also present the efficiency of the latter without overlap. In the case of the free Schrödinger equation, the quasi-optimal algorithm coincides with the optimal one and converges in two iterations as expected by the theory (see Theorem 3.1).

7.1.1. The classical Schwarz algorithm

The mesh Δx and Δt are fixed, equal to $\Delta x = 0.1$ and $\Delta t = 0.01$. The overlap is equal to eight gridpoints, i.e. to 0.8. We compute a Gaussian traveling wave

$$u(x, t) = \frac{e^{-i\pi/4}}{\sqrt{4t - i}} \exp\left(\frac{ix^2 - kx - k^2t}{4t - i}\right) \quad (7.1)$$

with $k = 6$, using the Crank–Nicolson scheme on (a, b) with the exact values as Dirichlet and initial data (transparent boundary conditions could be considered as well, but would give the exact discrete solution for constant potential only). We study in Fig. 1 the variation of the discrete L^2 error on the internal boundary of Ω_2 , $\sum_n |W_2^k(0, n)|^2$ as a function of the iteration number, for various final times T .

We notice two parts in the convergence curve: in the first iteration, the error decays very slowly. This is due to the Dirichlet boundary conditions which create fictitious walls. High amplitude waves are created by erroneous boundary data, and the maximum of the amplitude is reached at the end of the time interval. At each iteration, the error is small on a longer time interval. At some iteration (which increases with T), the error is small on the whole time interval, which makes the total error small.

In Table 1, we choose $T = 1$, and give the number of iterations needed to reach a precision equal to 10^{-6} for various sizes of the overlap from two to 16 gridpoints. As expected, the larger the overlap, the faster the algorithm. Furthermore, the numerical convergence factor is a linear function of the overlap.

7.1.2. The optimized complex Robin algorithm with overlap

From now on, we consider the convergence to zero, with a random initial datum on the interface. The final time is $T = 1$, the mesh sizes are equal to $\Delta x = 0.1, \Delta t = 0.01$, and thereafter divided by two, the overlap is equal to $4\Delta x$. The optimal p given by the

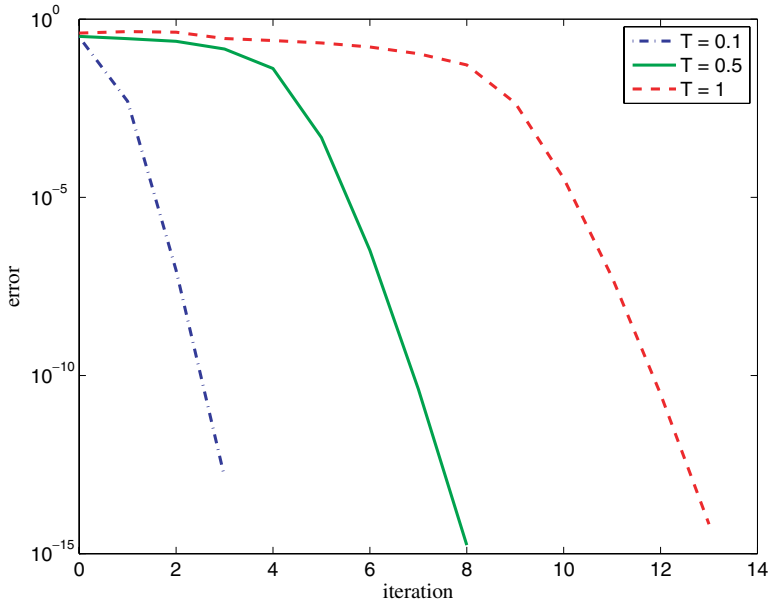


Fig. 1. Convergence history of the classical Schwarz algorithm for various values of the final time.

Table 1. Number of iterations to achieve a 10^{-6} accuracy as a function of size of the overlap for the classical Schwarz algorithm with $T = 1$.

Overlap	$2\Delta x$	$4\Delta x$	$8\Delta x$	$10\Delta x$
Number of iterations	54	27	14	7

theory is $p_T = (\frac{\pi^2}{T\Delta t})^{1/4} \sim 5.6$. We draw on Fig. 2 the L^2 error in Ω_1 at step 10 as a function of p . The star corresponds to p_T . This drawing shows that the efficiency of the complex Robin algorithm depends drastically on the parameter p , that the theoretical estimate is perfectly relevant, and that it is better to overestimate p than to underestimate. Figure 3 shows the equivalences of the log of the discrete L^2 error in time and space, for a range of values of $\Re p$ and $\Im p$. It shows that adding an imaginary part to p does not improve the efficiency of the algorithm.

7.1.3. Comparison

We now compare the efficiency of the classical and optimized complex Robin algorithm for $T = 1$, $\Delta x = 0.1$ and $\Delta t = 0.01$. The error is the L^2 norm of the error on the boundary of Ω_2 . The overlap is 4% or 8%, with the same data as in Fig. 3. The convergence of the optimized complex Robin algorithm is linear, and the improvement over the classical Schwarz algorithm is striking.

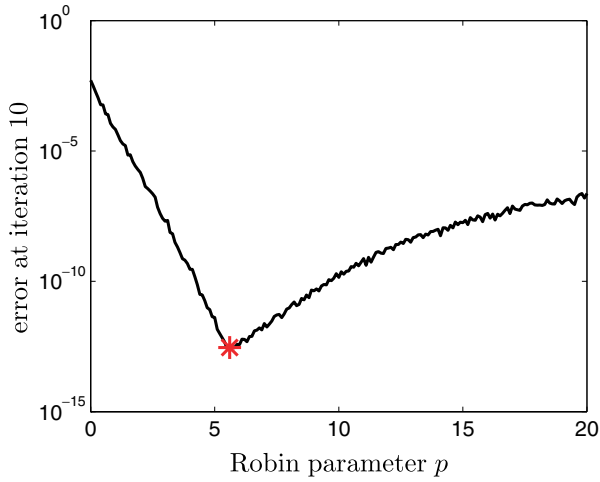


Fig. 2. Variation of the discrete L^2 error in time and space in Ω_1 as a function of p , logarithmic scale. The overlap is 1%. The star corresponds to the theoretical optimal value p_T .

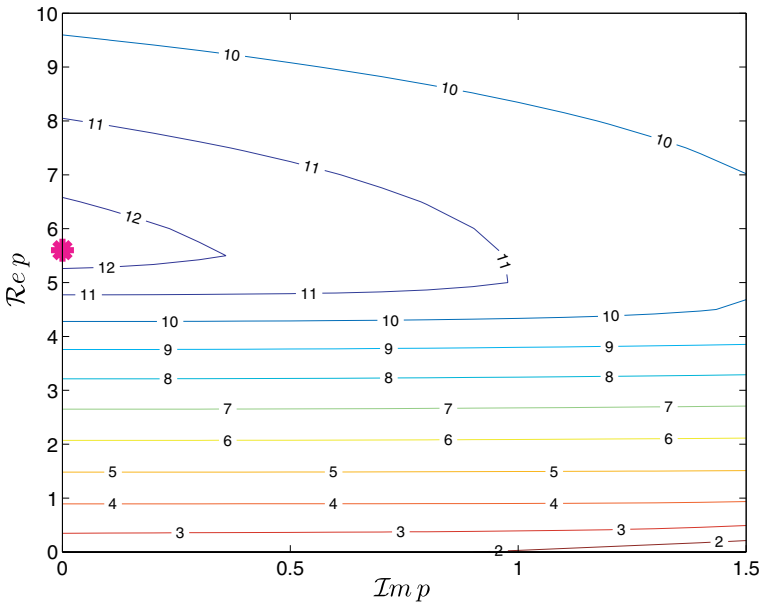


Fig. 3. Variation of the discrete L^2 error in time and space as a function of p , logarithmic scale. The overlap is 4%. The star corresponds to the theoretical optimal value p_T .

7.1.4. The optimized complex Robin algorithm without overlap

We now analyze the efficiency of the non-overlapping complex Robin algorithm. For the same data as before ($T = 1$, $\Delta x = 0.1$ and $\Delta t = 0.01$), Fig. 5 shows on the left the discrete L^2 error in time and space in Ω_1 after ten iterations as a function of p .

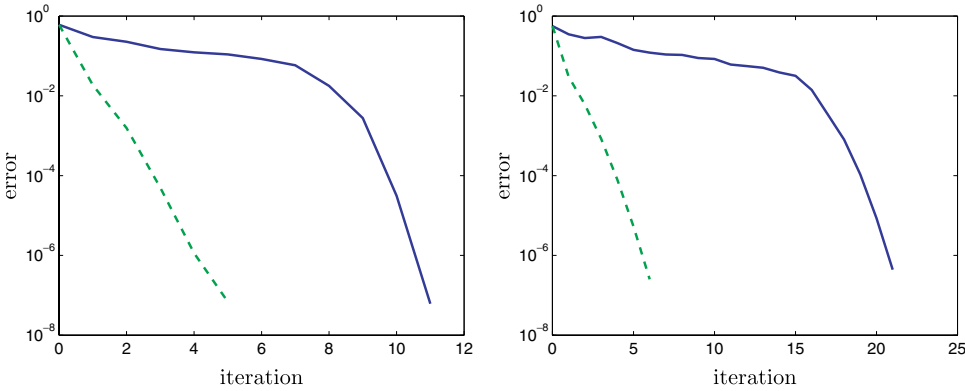


Fig. 4. Convergence history: Comparison of the Dirichlet (solid) and optimized complex Robin algorithm (dashed). The overlap is $L = 8\Delta x$ on the left, $L = 4\Delta x$ on the right.

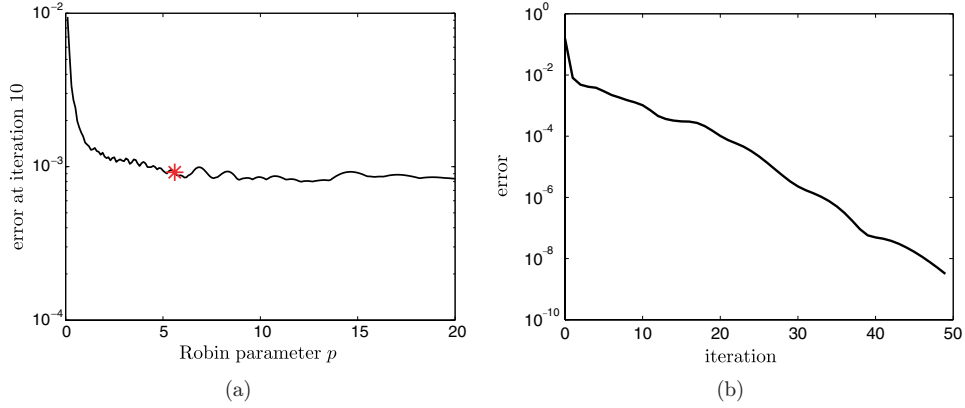


Fig. 5. (a) Error at iteration 10 as a function of p , (b) error history in logarithmic scale for the optimal theoretical parameter p^* .

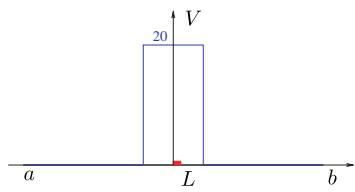


Fig. 6. Description of the data: Interval of computation, overlap, and potential.

The error is much larger than in the overlapping case, and much less sensitive to p . However, the optimal theoretical parameter p^* is included in the “best” region. We show on the right the variation of the error at the interface as a function of the iteration for $p = p^*$. The Jacobi algorithm damps rapidly the propagating modes first, and then

slows down. The convergence is therefore slower than in the overlapping case. This is due to the fact that there is no overlap to dampen the evanescent modes. As in the overlapping case, the convergence is linear, adding an imaginary part to p does not improve the convergence. If possible, a small overlap is preferable for improved convergence.

7.2. The potential barrier

We consider again the interval $(-5, 5)$, with a final time $T = 1$, discretized with $\Delta x = 0.1$ and $\Delta t = 0.01$. The size of the overlap is $4\Delta x$. The potential is 20 times the characteristic function of the interval $(-1, 1)$.

We use the optimization process of Sec. 4.4, for a constant potential V equal to 20. The theoretical formula in Halpern–Szeftel¹² gives a theoretical parameter p^* equal to 4.64.

In the experiment, again the initial data is zero, and the initial guess on the boundary is random. We draw in Fig. 7 on the left the error at iteration 5 as a function of p . The star corresponds to the theoretical optimal value p^* . The numerical best value is $p_d = 4.93$. We see that the numerical result fits very well with the theoretical analysis. Figure 7 on the right compares the convergence history for Dirichlet and complex Robin transmission with parameter p^* . In this case, the improvement produced by the optimized complex Robin condition is even larger than in the case of the free Schrödinger equation in Fig. 4 on the right.

We tried various types of potential, like parabolic profiles and the results are the same: The complex Robin algorithm behaves much better than the classical Schwarz, and the optimal complex Robin is obtained for a value of the parameter of the same order of magnitude as the theoretical one.

7.3. The quasi-optimal algorithm

The quasi-optimal algorithm is by far the most efficient. In all cases, even when the potential is not constant, the precision 10^{-12} is reached in at most five iterations with or without overlap. As an example, we show in Fig. 8 the convergence history with an overlap of four gridpoints, for a parabolic potential, for various mesh sizes. When refining the mesh, the first two iterations reduce the error less, but after four iterations the error is about 10^{-12} . In that sense we can say that the convergence is almost independent of the mesh size. In Fig. 9, we show the first few iterations, at the end of the time interval, of the quasi-optimal algorithm with a parabolic potential, in the case where $\Delta x = 0.05$ and $\Delta x = 0.005$.

7.4. The case of many subdomains

Although the mathematical analysis was carried out in the simplified case of two semi-infinite intervals, the proofs of convergence remain unchanged for an arbitrary number of subdomains in the non-overlapping case.

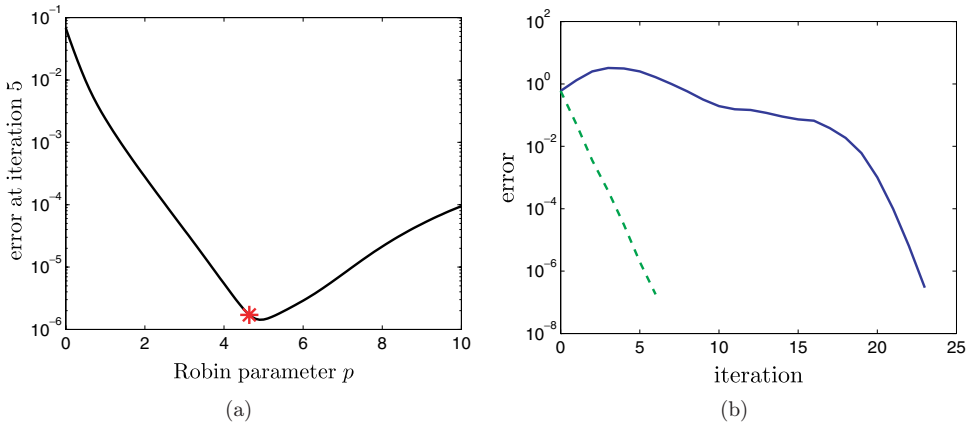


Fig. 7. (a) Error at iteration 5 for the complex Robin algorithm as a function of p . (b) Convergence history for Dirichlet (solid) and complex optimized Robin (dashed) algorithms. Potential barrier.

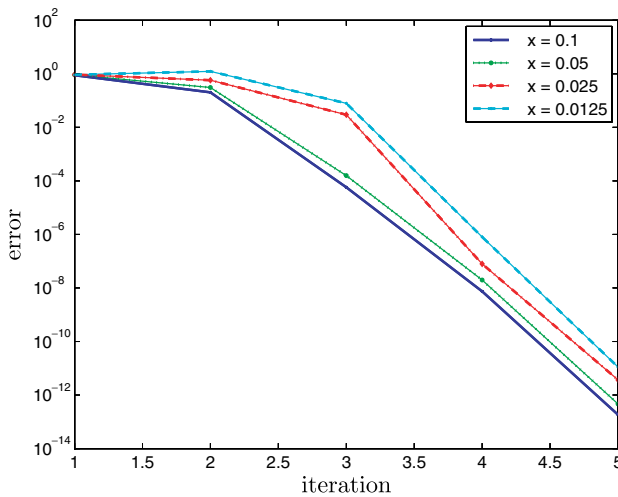


Fig. 8. Convergence history for the quasi-optimal algorithm in the presence of a parabolic potential.

In Figs. 10 and 11 are two sets of experiments, carried on the time interval $(0, 1)$, for four to 20 subdomains of same size equal to ten gridpoints. The numerical data are $\Delta x = 0.1$, $\Delta t = 0.01$. The error is the sum of the errors on the interfaces. In Fig. 10 the potential is zero. The convergence does not depend on the number of subdomains. In Fig. 11, the potential is $10x^2$. The convergence curves are parallel in each case, there is a factor ten in the error between the extreme curves. For 20 subdomains, we need eight iterations to reach 10^{-10} with the complex Robin algorithm, and only five iterations with the quasi-optimal. The quasi-optimal algorithm is therefore the most effective in all cases. However, we must keep in mind that it is global in time on the boundary, and therefore each iteration involves the computation of N coefficients.

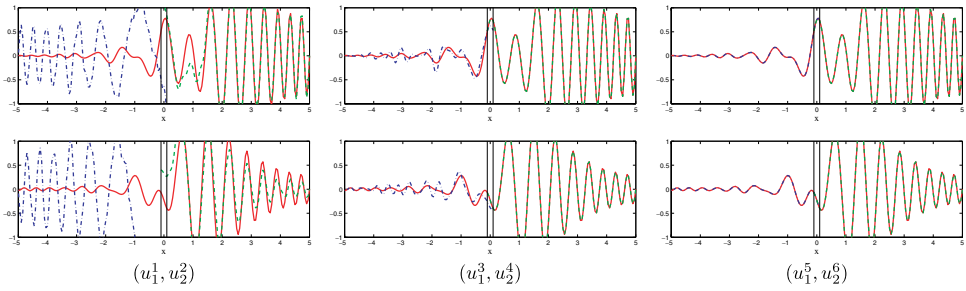


Fig. 9. From left to right, the iterates $u_1^k(x, T)$ and $u_2^{k+1}(x, T)$ (dashed) at the end of the time interval $t = T$ for $k = 1, 3, 5$, together with the exact solution (solid), for the quasi-optimal algorithm. Top: real part, bottom: imaginary part. Parabolic potential.

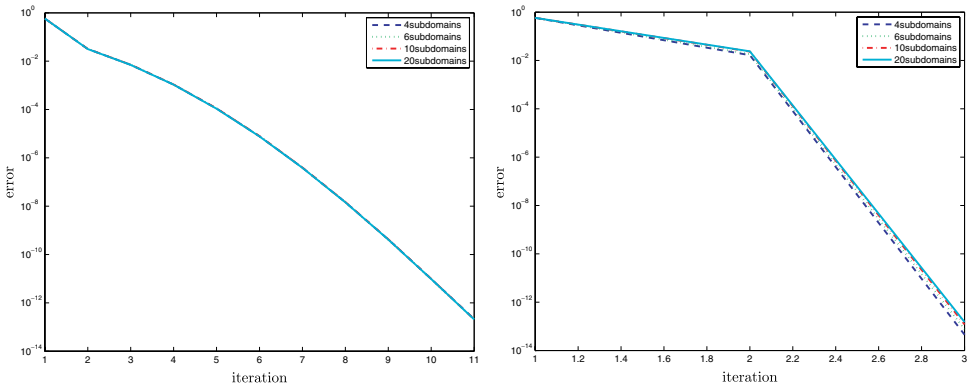


Fig. 10. Convergence history for the free Schrödinger equation, for various number of subdomains. (a) Complex Robin, (b) quasi-optimal.

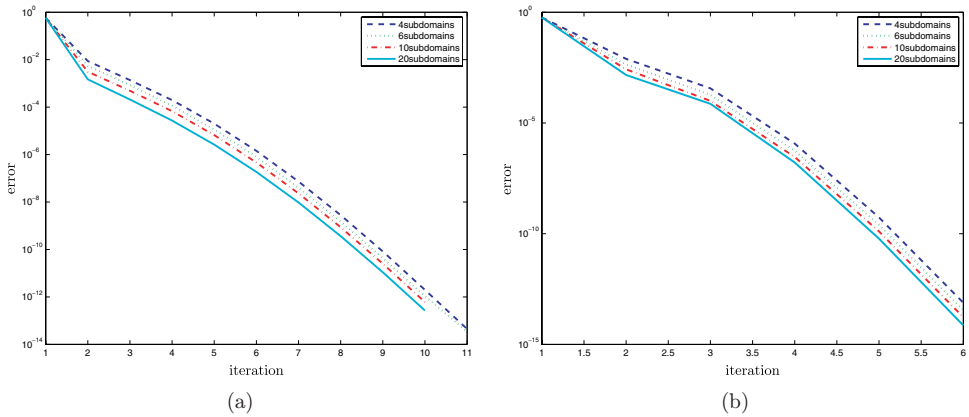


Fig. 11. Convergence history for the Schrödinger equation with a parabolic potential, for various number of subdomains. (a) Complex Robin, (b) quasi-optimal.

As an example, in MATLAB, without any optimization of the code, in the case of two subdomains and $T = 1$, we found that for $\Delta x = 0.1$, $\Delta t = 0.01$, the Robin algorithm and the quasi-optimal algorithm have about the same cost, whereas for $\Delta x = 0.025$, the quasi-optimal algorithm is three times more costly than the Robin algorithm. However, optimal implementations of the Transparent Boundary Conditions can be used, like the one of Lubich and Schädle.¹⁷

8. Conclusion

We presented a general approach to design optimized Robin and quasi-optimal domain decomposition algorithms for the linear Schrödinger equation, with a potential in one dimension. We established a complete analysis of those, and showed numerical examples with various types of potential, which enhance the efficiency of the methods. These algorithms can be used with or without overlap. This work is a first step towards the extension to the two-dimensional case, and to the nonlinear Schrödinger equation.

References

1. X. Antoine, A. Arnold, C. Besse, M. Ehrhardt and A. Schädle, A review of transparent and artificial boundary conditions techniques for linear and nonlinear Schrödinger equations, *Commun. Comput. Phys.* **4** (2008) 729–796.
2. A. Arnold and M. Ehrhardt, Discrete transparent boundary conditions for the Schrödinger equation, *Riv. Math. Univ. Parma* **6** (2001) 57–108.
3. A. Arnold, M. Ehrhardt and M. Schulte, *Very-Large-Scale Integration (VLSI): Architecture, Performance and Nano Applications* (Nova Publishers, 2008).
4. D. Bennequin, M. J. Gander and L. Halpern, A homographic best approximation problem with application to optimized Schwarz waveform relaxation, *Math. Comp.* **74** (2009) 185–223.
5. P. D’Anfray, L. Halpern and J. Ryan, New trends in coupled simulations featuring domain decomposition and metacomputing, *M2AN* **36** (2002) 953–970.
6. B. Després, Méthodes de décomposition de domaines pour les problèmes de propagation d’ondes en régime harmonique, Ph.D. thesis, Université Paris IX Dauphine, 1991.
7. B. Engquist and H. K. Zhao, Absorbing boundary conditions for domain decomposition, *Appl. Numer. Math.* **27** (1998) 341–365.
8. M. J. Gander and L. Halpern, Absorbing boundary conditions for the wave equation and parallel computing, *Math. Comp.* **74** (2004) 153–176.
9. M. J. Gander and H. Zhao, Overlapping Schwarz waveform relaxation for parabolic problems in higher dimension, in *Proc. of Algoritmy 14*, eds. A. Handlovičová, M. Komorníková and K. Mikula (Slovak Technical University, September 1997).
10. M. J. Gander, L. Halpern and F. Nataf, Optimal Schwarz waveform relaxation for the one-dimensional wave equation, *SIAM J. Num. Anal.* **41** (2003) 1643–1681.
11. L. Halpern, Local space time refinement for the wave equation, *J. Comp. Acoustics* **13** (2005) 153–176.
12. L. Halpern and J. Szeftel, Optimized and quasi-optimal Schwarz waveform relaxation for the one-dimensional Schrödinger equation, Technical Report, <http://hal.ccsd.cnrs.fr/ccsd-00067733>, CNRS, 2006.

13. C. Japhet, Optimized Krylov–Ventcell method, Application to convection-diffusion problems, in *Proc. of the 9th Int. Conf. on Domain Decomposition Methods*, eds. P. E. Bjørstad, M. S. Espedal and D. E. Keyes (ddm.org, 1998), pp. 382–389.
14. J.-L. Lions and E. Magenes, *Problèmes aux Limites Non Homogènes et Applications*, Travaux et recherches mathématiques, Vols. 17 and 18 of (Dunod, 1968).
15. P.-L. Lions, On the Schwarz alternating method, I. In *First Int. Symp. on Domain Decomposition Methods for Partial Differential Equations*, eds. R. Glowinski, G. H. Golub, G. A. Meurant and J. Périaux (SIAM, 1988), pp. 1–42.
16. P.-L. Lions, On the Schwarz alternating method, III: A variant for non-overlapping subdomains, in *Third Int. Symp. on Domain Decomposition Methods for Partial Differential Equations*, Houston, Texas, March 20–22, 1989 (SIAM, 1990).
17. C. Lubich and A. Schädle, Fast convolution for non-reflecting boundary conditions for Schrödinger-type equations, *SIAM J. Sci. Comput.* **24** (2002) 161–182.
18. F. Nataf and F. Nier, Convergence of domain decomposition methods via semiclassical calculus, *Comm. Partial Differential Equations* **23** (1998) 1007–1059.
19. F. Nataf, F. Rogier and E. de Sturler, Optimal interface conditions for domain decomposition methods, Technical Report 301, CMAP (École Polytechnique), 1994.
20. W. Rudin, *Real and Complex Analysis* (McGraw-Hill, 1966).
21. H. A. Schwarz, Über einen Grenzübergang durch alternierendes Verfahren, *Vierteljahrsschrift Naturforschenden Gesellschaft* **15** (1870) 272–286.
22. J. C. Strikwerda, *Finite Difference Schemes and Partial Differential Equations* (Chapman and Hall, 1989).